Aus dem Institut für Physiologie und Pathophysiologie
Geschäftsführender Direktor: Prof. Dr. Dominik Oliver
des Fachbereichs Medizin der Philipps-Universität Marburg

Regulation of TASK potassium channels by G-protein coupled receptors

Inaugural-Dissertation zur Erlangung
des Doktorgrades der Naturwissenschaften

dem Fachbereich Medizin der Philipps-Universität Marburg
vorgelegt von
Bettina Ulrike Wilke aus Chemnitz

Marburg, 2017

Angenommen vom Fachbereich Medizin der Philipps-Universität Marburg am: 21.03.2017

Gedruckt mit Genehmigung des Fachbereichs.

Dekan: Prof. Dr. Helmut Schäfer
Referent: Prof. Dr. Dominik Oliver
Korreferent: Prof. Dr. Timothy Plant

Anmerkung

Für die vorliegende Doktorarbeit beziehe ich mich auf §9 der „Promotionsordnung der Mathematisch-Naturwissenschaftlichen Fachbereiche und des Medizinischen Fachbereichs für seine mathematisch-naturwissenschaftlichen Fächer der Philipps-Universität Marburg vom 15.07.2009“, wonach eine wissenschaftliche Publikation als Dissertationsleistung anerkannt werden kann. Somit enthält diese Arbeit, neben einer Einleitung und einer Diskussion, eine Zusammenfassung der Ergebnisse folgender Publikation:

Bettina U. Wilke, Moritz Lindner, Lea Greifenberg, Alexandra Albus, Yannick Kronimus, Moritz Bünemann, Michael G. Leitner, and Dominik Oliver. Diacylglycerol mediates regulation of TASK potassium channels by Gq-coupled receptors. *Nat Commun*. 2014 Nov 25;5:5540. doi: 10.1038/ncomms6540

Die Angabe meines Anteils an dieser Veröffentlichung findet sich unter Gliederungspunkt „3 - My contribution to the presented article“ auf Seite zwölf.

Zusammenfassung

TASK Kaliumkanäle tragen in vielen Zelltypen zur Generierung des Membranpotentials bei, wodurch sie zahlreiche zelluläre Funktionen beeinflussen. Obwohl TASK-vermittelte Ströme häufig als „Hintergrundleitfähigkeit“ bezeichnet werden, sind sie vielfach reguliert; unter anderem werden TASK Kanäle durch jene Hormone und Neurotransmitter gehemmt, welche Gαq/11-Protein-gekoppelte Rezeptoren (GqPCR) aktivieren. Diese Kanalregulation spielt zum Beispiel für die Anpassung der Erregbarkeit von Nerven- und Herzmuskelzellen, wie auch für die Aldosteronsekretion in der Nebenniere eine Rolle. Trotz der physiologischen Bedeutung von TASK Kanälen und deren Inhibition konnte der zugrunde liegende Mechanismus für die GqPCR-vermittelte Regulation noch nicht aufgeklärt werden. Die vorliegende Arbeit hat zum Ziel, das verantwortliche Signalmolekül zu identifizieren und seinen Effekt auf zerebelläre Körnerzellen zu untersuchen.

Die klassische GqPCRs Signalkaskade beginnt mit der Aktivierung von Gαq, welches die Phospholipase Cβ aktiviert. Diese spaltet daraufhin das Membranlipid Phosphatidylinositol(4,5)bisphosphat zu Diacylglycerol (DAG) und Inositol(1,4,5)trisphosphat. Mit verschiedenen experimentellen Ansätzen habe ich zuerst die Bedeutung der Phospholipase C für die GqPCR-vermittelte TASK Regulation herausgearbeitet. In weiterer Folge konnte ich zeigen, dass die direkte Applikation eines DAG-Analogons ausreicht, um den Kanal zu inhibieren. Die Abschwächung des durch Stimulation von GqPCRs erreichten DAG-Transienten durch Überexpression DAG-metabolisierender Enzyme reduzierte gleichermaßen die Inhibition der TASK Kanäle. Da bereits gezeigt wurde, dass ein sechs Aminosäuren langes Motiv im TASK C-Terminus essentiell für die GqPCR-vermittelte Inhibition ist, habe ich den Kanal in diesem Motiv mutiert und die Mutanten auf ihre DAG-Sensitivität untersucht. Die Ergebnisse zeigen eine Korrelation zwischen der Inhibition durch Aktivierung eines GqPCRs und der Applikation des DAG-Analogons und untermauern die vorangegangenen Resultate, dass die DAG Produktion der GqPCR-vermittelten TASK Inhibition zugrunde liegt. Um die Ergebnisse aus den heterolog exprimierenden Zellen im nativen System zu validieren, untersuchte ich den TASK-vermittelten Strom IK_{SO} in dissoziierten zerebellären Körnerzellen. Sowohl die Aktivierung muskarinischer Rezeptoren, als auch die Applikation des DAG-Analogons führten zu einer deutlichen Reduktion des IK_{SO}, welche mit einer Depolarisation der Zellmembran einher ging.

Zusammengefasst zeigen meine Ergebnisse, dass DAG der verantwortliche *second messenger* in der GqPCR Signalkaskade ist, welcher zur Schließung der TASK Kanäle führt. Das erweitert die Sicht auf die Signalwirkung des kleinen Membranlipids DAG und betont den Zusammenhang zwischen DAG und zellulärer Erregbarkeit.

Summary

TASK potassium channels control the membrane potential in many cell types and thus affect a plethora of cellular functions such as excitability of neurons and cardiac muscle, and secretion of aldosterone in the adrenal gland. Although commonly termed 'leak channels', TASK channels are highly regulated. Most importantly, they are strongly inhibited by a variety of hormones and neurotransmitters activating Gq-protein coupled receptors (GqPCRs). Despite extensive studies of TASK inhibition by the GqPCR-induced signaling cascade, the underlying mechanism of channel regulation has not been elucidated. Thus I aimed to unravel the second messenger responsible for GqPCR-mediated TASK channel inhibition and validate my findings from the heterologous expression system in cerebellar granule neurons.

The signaling cascade induced by GqPCRs is initiated by activation of Gαq, which in turn stimulates phospholipase Cβ to hydrolyze the membrane phospholipid phosphatidylinositol(4,5)bisphosphate producing the second messengers 1,2-diacylglycerol (DAG) and inostol(1,4,5)trisphosphate. Using different approaches, I first established that phospholipase C is critical for GqPCR-mediated TASK channel inhibition. Next, I found that direct application of a DAG analog was sufficient to inhibit TASK channels. Accordingly, experimental attenuation of the DAG transients evoked by GqPCR stimulation diminished TASK channel inhibition, indicating that DAG is responsible for the current reduction following receptor activation. Because it had been previously established that a six amino acid motif within the proximal C-terminus is important for TASK channel regulation by GqPCRs, I compared the effects of GqPCR stimulation and DAG application on TASK channel proteins either truncated or mutated within this motif. A correlation of the sensitivities towards DAG and GqPCR activation further supported the hypothesis of DAG production as the underlying mechanism for the GqPCR-mediated effect. Lastly, to test whether native TASK-mediated currents were also inhibited by DAG, I probed application of this lipid on dissociated cerebellar granule neurons that express the TASK-mediated standing outward potassium current (IK_{SO}). IK_{SO} was inhibited by muscarinic receptor agonist as well as by direct application of DAG, producing a significant membrane depolarization.

In conclusion, my findings demonstrate that DAG mediates the GqPCR-induced inhibition of TASK channels in an expression system as well as native, TASK-mediated currents. Thus, my data expand the view on the signaling effects of the small membrane lipid DAG and establish a link between DAG and cell excitability. Additionally, they may pave the way towards understanding the mechanism of DAG action on ion channels as atypical DAG effector proteins.

Table of contents

1 Introduction

Excitability of cells depends on the plasma membrane conductance for potassium, which is critical for 1) maintaining a negative membrane potential, 2) fast repolarization facilitating high-frequency firing in neurons, and 3) controlling the impact of excitatory input by reducing the membrane resistance. The large number of potassium channels that have evolved to accomplish these diverse tasks can be grouped in voltage-dependent six-transmembrane-domain (TMD) potassium channels, inward rectifiers and the two-pore-domain potassium channels (K2P)[33,49]. The subunits of K2P channels consist of four TMDs with two pore-loops in tandem. Functionally, they have often been referred to as simple 'leak' or 'background' channels[36]. However, they are highly regulated by a plethora of stimuli as diverse as membrane stretch, intra- and extracellular pH, volatile anesthetics, Gq-protein coupled receptors (GqPCR), and the electrochemical driving force[30,59,64,87]. In the following section I will outline some of the features of K2P channels.

1.1 Characteristics of K2P channels

In mammals, 15 potassium channel subunits share the typical two-pore topology and thus belong to the K2P channel family. According to the HUGO gene nomenclature, KCNK1-18 (leaving out KCNK8, -11, and -14) are their assigned genomic names, giving rise to potassium channel proteins termed K2pX.1 (with X being the number in the gene name). Alternatively, they are commonly found in literature under their trivial abbreviations derived from 'Tandem of P-domains in weak inward rectifier potassium channel' (TWIK), which I will use in my thesis. K2P channel proteins were classified into six subfamilies according to sequence similarity: TWIK, TREK, TALK, THIK, TRESK, and TASK (TWIK-related acid sensitive potassium channel; for the other names see list of abbreviations)[30,59]. In this work I will focus on the latter subfamily, comprising of the members TASK1 and TASK3, characterized by their inhibition by acidic pH and by GqPCRs, as well as their activation by volatile anesthetics[15,28,43,47,76,81,96]. The third member of this family, TASK5, does not yield functional channels in heterologous expression systems and its physiological function is unknown[42].

Insights into the structural characteristics of K2P channels were recently gained from crystal structures of TWIK1[69], TRAAK[11,12], and TREK2[27]. K2Ps consist of two pore-forming P-loops, which contain the selectivity filter identifiable by the consensus amino acid sequence T-X-G-Y/F/L-G (see figure 1). As four P-loops are necessary to form a functional channel pore, K2P subunits assemble as dimers[36]. In addition to homodimerization, heterodimerization of subunits within and in between subfamilies was described in heterologous expression systems and native tissue[6,8,22,46,51,79,84].

Dimerization critically depends on the extracellular cap formed by two short α-helices between the first two transmembrane domains. This distinctive feature of K2P channels leads to subunit interaction either through a disulfide bond or hydrophobic interactions[32,48]. Additionally, it contributes to the extracellular ion pathway, which allows for potassium passage from the channel's selectivity filter to the extracellular medium[32,34].

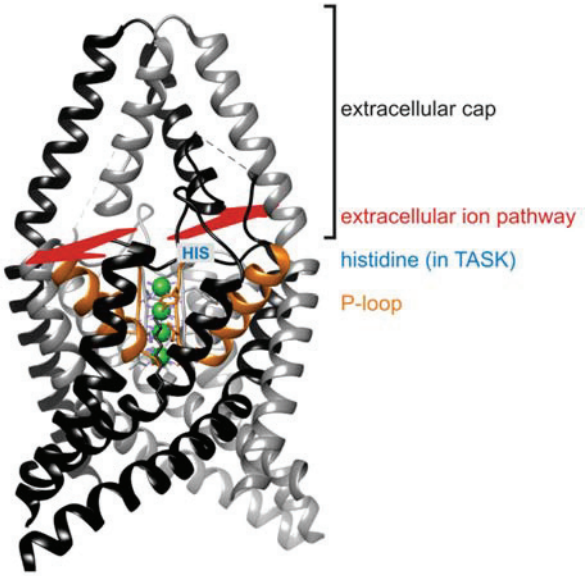

Figure 1: TREK2 crystal structure to visualize characteristics of K2P channels. A ribbon model of TREK2 formed by two subunits (black and grey) is depicted. The P-loops (orange) contain the selectivity filter, containing four binding sites for potassium (represented as green spheres). Potassium leaves the channel through the extracellular ion pathway (red). A histidine (blue) not present in TREK2 is found in TASK and confers pH-sensitivity to these channels. The structure was modified from protein database ID 4BW5 published by Dong et al. (2015)[27].

Despite these structural insights, channel gating has not been completely resolved yet. However, gating critically involves the selectivity filter of K2P channels[87]. It is thought that the inactive selectivity filter is ion-deprived and gating depends on the ion occupancies of the distinct potassium binding sites within the conduction pathway[34,87]. Protonation of a histidine adjacent to the selectivity filter (see figure 1) is responsible for the pH sensitivity of TASK1 and TASK3 by reducing the width of the extracellular ion permeation pathway and by destabilizing the coordination of the potassium ion at the outermost binding site of the selectivity filter[34,81]. In addition to pH, also the electrochemical driving force for the permeant ion gates the channel, because ion occupancy of the filter and outward ion flux facilitate the conductive state of the channel[87]. In contrast to classical voltage-dependent potassium channels, inactivation of K2P channels is typically not found. This indicates that the canonical 'C-type gate' responsible for C-type inactivation in voltage-gated potassium channels is either inversely coupled to channel activation or only modulated by direct regulators[5,20,25,104]. The presence of a functional inner activation gate in K2P channels, equivalent to the helix-bundle crossing in voltage-gated potassium channels, is contentious and may not play a role in physiological channel gating[2,5,78].

1.2 Cellular role and functional importance of TASK1/3

The biophysical properties of TASKs suggest a vast impact of these channels on the electrical characteristics of cells. Because TASK channels mediate significant potassium conductances at negative potentials, they contribute to setting the resting membrane potential close to the potassium equilibrium potential and conduce to input resistance[19,96]. Additionally, like most other K2P channels, both TASK1 and TASK3 show time-dependent voltage activation[87]. Together with a lack of inactivation, this promotes repolarization in excitable cells even at sustained high frequency firing by fast repolarization of the membrane potential after action potential firing[62,82]. In native tissue, this has been demonstrated most convincingly in cerebellar granule neurons (CGNs)[10]. These cells express a standing outward potassium current (IK_{SO}) at depolarized poten-

tials, which is mediated by TASK1/3[1,10,35,40,68]. Significant current reduction was seen in TASK3 knockout CGNs, leading to broader action potentials of reduced amplitude together with strong action potential accommodation during supra-threshold current injections[10]. Analogously, acute IK_{SO} inhibition increased the input resistance and excitability of these CGNs[19,102]. The high abundance[97] and important cellular role of TASK1 and TASK3 in CGNs (as well as in motoneurons) explains the involvement of TASK channels in motor control found in knockout studies[54]. A similar importance of TASK channels on neuronal excitability is evident in thalamocortical relay neurons. In these cells, TASK inhibition by stimulation of muscarinic acetylcholine receptors can switch the firing pattern from bursting to single spike firing, which is associated with sleep-wake transition[67].

In addition to the role of TASK channels in the central nervous system, these proteins also control many cellular functions in the periphery by influencing the electrical membrane properties. To give two examples, I like to mention the heart, where TASK1 is of clinical relevance reducing the action potential duration[80,88]. In the adrenal cortex, angiotensin II receptor modulation of TASK channels is involved in controlling aldosterone secretion[4].

1.3 Regulation of TASK1/3

Besides their vast expression pattern and importance for the electrical properties of cells, the relevance of TASK channels is further highlighted by their regulation by diverse stimuli. As their name 'TWIK-related acid-sensitive potassium channel' indicates, extracellular acidification in the physiological range closes the channels (pK of 7.3 for TASK1 and 6.7 for TASK3, while TASK1/3 heteromers show intermediate pH sensitivity)[22,28,43]. Relevant pH changes occur for example during exocytosis, ischemia, and seizures[50,82], yet the role of TASK channels during these (patho-)physiological processes remains to be elucidated. In addition to protons, extracellular divalent cations like calcium, magnesium and zinc also inhibit TASK3[19,71]. Furthermore, activation of the neuronally widely expressed TASK channels by the volatile anesthetics halothane and isoflurane may contribute to the anesthetic effects of these drugs, stressing the clinical relevance of these ion channels[53,76,90,98].

Apart from direct effects of the aforementioned chemical activators or inhibitors, endogenous TASK currents are modulated by hormones and neurotransmitters that activate seven-transmembrane-domain receptors coupled to Gαq/11[96]. Despite intense efforts, the second messenger responsible for this inhibition is still under debate[17,18,23,55]. In the next section I will outline the signaling cascade initiated by activation of these GqPCRs and the second messengers possibly involved in TASK channel regulation.

1.4 GqPCR signaling and second messengers implicated in TASK regulation

Seven-transmembrane-domain receptors coupled to heterotrimeric G-proteins (consisting of the subunits Gα and the obligatory dimer Gβγ) are the most diverse plasma membrane receptors[7]. Upon activation, these receptors initiate an exchange of guanosindiphosphate (GDP) for guanosintriphosphate (GTP) in Gα subsequently inducing dissociation of Gα and Gβγ, which in

turn leads to effector response[83]. The signaling specificity mainly depends on the Gα subunits involved (4 subfamilies: Gαs, Gαi, Gα12/13, Gαq/11)[66]. Due to the fact that signaling effects for Gβγ require high dimer concentrations only achieved by Gαi signaling, I will neglect this part of the signaling path[39]. As TASK channels are inhibited specifically by Gαq/11-coupled receptors[1,23,68,96,100], I will focus on the signaling events evoked by GqPCRs in the following (see figure 2).

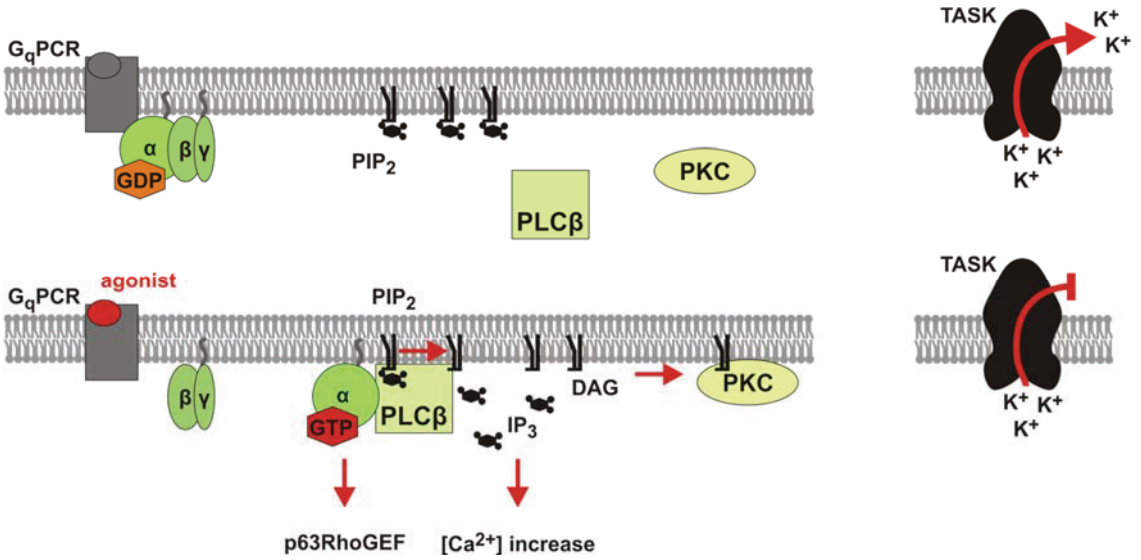

Figure 2: Schematic presentation of the signaling cascade elicited by GqPCRs. Stimulation of GqPCRs activates various effectors and causes inhibition of TASK channels. See text for further description.

The major effector of activated Gαq is phospholipase Cβ (PLCβ)[56]. PLCβ hydrolyses the membrane lipid phosphatidylinositol(4,5)bisphosphate (PIP_2) to release inositol(1,4,5)trisphosphate (IP_3) and 1,2-diacylglycerol (DAG)[39]. However, Gαq can also elicit downstream effects independently of PLC via p63RhoGEF[61], which activates RhoA and thus links Gαq signaling to actin cytoskeleton dynamics, but data on the role of this pathway for TASK channel regulation are ambiguous[18,88,89]. Additionally, activated Gαq itself has been shown to inhibit the unselective cation channel TRPM8 via direct interaction[103]. Based on two key experiments, Chen *et al.* (2006) postulated that Gαq also directly regulates TASK channel activity without involvement of PLC[18]: They elicited TASK inhibition 1) by activating a Gαq mutant protein presumably deficient in PLC coupling and 2) through active Gαq despite pharmacological inhibition of PLC[18]. Based on these findings the authors concluded that Gαq directly inhibited TASK channels in response to GqPCRs and that signaling molecules downstream of Gαq generated by PLC were not involved in this process. However, contradicting the results from Chen *et al.* (2006), several groups found that PLC is both necessary and sufficient for GqPCR-mediated TASK inhibition[17,23,88]. Specifically, pharmacological inhibition of PLC by the well established antagonist U73122 was performed in many studies, and all with the exception of two[9,18] found impaired GqPCR-induced TASK regula-

tion with this compound[17,23,88]. Additionally, activation of PLCβ2 via Gβγ liberated from Gαi-coupled receptors was sufficient to inhibit TASK1 currents[23].

The PLC substrate PIP_2 serves as a precursor for the signaling phospholipid phosphatidylinositol(3,4,5)trisphosphate (PIP_3) and regulates various membrane proteins itself[75,94]. In particular, it is well established that the activity of many ion channels, including voltage-gated and inward-rectifier potassium channels, depends on PIP_2 levels[85,95]. This gave rise to the idea that GqPCR-mediated TASK channel inhibition may also be due to PIP_2 depletion. Indeed, some evidence pointed to PIP_2 dependence of TASK channels[17,23,57], but using sophisticated genetically encoded tools to acutely deplete distinct phosphoinositides in live cells, Lindner *et al.* (2011) refuted the hypothesis that sole phosphoinositide depletion could lead to TASK channel inhibition[55].

Besides the PLC substrate PIP_2, the hydrolysis products IP_3 or DAG and their evoked signaling pathways have also been analyzed as candidate mediators responsible for TASK inhibition by GqPCRs. The freely diffusible IP_3 activates endoplasmic calcium channels, which subsequently cause an increase in cytosolic calcium concentration[93]. Several lines of evidence argue against an effect of calcium on TASK channels[23,43] and most results question the direct role of IP_3 on TASK[17,23]. Together with DAG, the store-operated calcium release contributes to activation of proteinkinase C (PKC)[72]. However, neither pharmacological intervention in PKC signaling[17,23], nor removal of all potential PKC phosphorylation sites in the TASK3 C-terminus pointed towards a crucial role of PKC in GqPCR-mediated TASK channel inhibition[100].

As for PKC, DAG modulates protein function by binding to C1-domains[13,14]. Additionally, DAG directly controls TRPC3/4/5/6 ion channels[37,92], which lack a C1-domain, and serves as a precursor for further signaling lipids: DAG can be hydrolyzed by DAG-lipases to monoacylglycerol, for example to the endocannabinoid 2-arachidonoylglycerol (2-AG)[29,37]. 2-AG can be further metabolized to signaling fatty acids like arachidonic acid (AA), which has been shown to inhibit TASK3 upon direct application to inside-out patches[43]. In a second metabolic pathway, DAG phosphorylation by DAG-kinases generates phosphatidic acid (PA), which can also signal on its own or serve as a substrate in lipid metabolism[29,37]. To my knowledge, a detailed analysis of DAG and its downstream effectors in GqPCR-mediated TASK channel inhibition has not been performed so far.

2 Aim

TASK channels control the membrane potential of many cell types and thus play a pivotal role for the function of neurons and peripheral organs. It is well established that TASK channel inhibition by numerous hormones and neurotransmitters is mediated by stimulation of GqPCRs and provides fast and reversible regulation of the electrical properties of many cell types. However, despite great efforts to understand the mechanism of this regulation, the involved second messenger has not been identified unequivocally so far. This thesis was conceived to identify the molecular mechanism that underlies TASK channel inhibition following receptor stimulation. To resolve the inconsistencies of previous studies and to comprehensively analyze TASK channel regulation, I examined the following aspects:

First, I scrutinized the relevance of PLC for GqPCR-mediated TASK inhibition and unraveled some of the problems that had led to contradicting results. To this end I evaluated TASK channel regulation subsequent to inhibition of PLC activity either by pharmacological block, by abrogation of physiological activation, or by depletion of the PLC substrate. Importantly, efficient manipulation of PLC signaling under my experimental conditions was validated using established sensors for PLC activity.

Second, I identified DAG as the responsible second messenger inhibiting TASK channels upon PLC activation. This was done by direct application of a DAG analog onto cells expressing TASK channels, thus excluding stimulation of other effectors within the signaling cascade. Further, I manipulated cellular dynamics of DAG with genetically-encoded tools to verify the relevance of DAG for mediating channel inhibition.

Third, I investigated the proximal TASK C-terminus for its role in GqPCR- and DAG-mediated channel inhibition. To this end I introduced several alanine and stop mutations within a short structural motif in TASK channels known to be critical for channel regulation. The good correlation between GqPCR and DAG sensitivity of these mutants corroborated the role of DAG as the responsible second messenger for GqPCR-mediated TASK inhibition and pointed to this regulatory six amino acid motif as the site of DAG action.

Finally, I aimed to test whether native TASK-mediated currents were inhibited by a similar mechanism. Given the pre-eminent importance of TASK channels for CGN development and function, I evaluated the DAG sensitivity of the TASK-mediated IK_{SO} found in CGNs and the impact of increased DAG levels on the resting membrane potential in these neurons.

3 My contribution to the presented article

I conceived this project together with Prof. Dr. Dominik Oliver based on preliminary work done by Dr. Moritz Lindner. I performed the experiments and analysis of the data presented in figure 1a-c, 1g-j, 2, 3a-c, 5b-f, 6 and 7. Dr. Moritz Lindner contributed to the graphs in figure 1 b and c and the EGTA data in figure 2b. During the course of their internships, the students Lea Greifenberg and Alexandra Albus were part of this project and contributed some of the measurements presented in Fig 6c and d after they were initially trained by me. Dr. Michael Leitner performed some of the measurements presented in figure 6b. I wrote and edited the manuscript and designed all figures together with Prof. Dr. Dominik Oliver.

4 Results

The results presented here were published in Nature Communications in 2014:

BETTINA U. WILKE, Moritz Lindner, Lea Greifenberg, Alexandra Albus, Yannick Kronimus, Moritz Bünemann, Michael G. Leitner, and Dominik Oliver. Diacylglycerol mediates regulation of TASK potassium channels by Gq-coupled receptors. *Nat Commun*. 2014 Nov 25;5:5540. doi: 10.1038/ncomms6540.

Figure references given in the results section refer to this article.

4.1 Role of PLC for GqPCR-mediated TASK channel inhibition

In order to distinguish between TASK channel inhibition directly by interaction with Gαq on the one hand and by second messengers resulting from PLC activity on the other hand, I first analyzed the involvement of PLC in GqPCR-mediated TASK inhibition by interfering with PLC activation or activity. In detail, I 1) blocked PLC pharmacologically, 2) impaired coupling of Gαq to PLC using Gαq mutants, 3) buffered intracellular calcium below levels required for PLC activity, and 4) depleted the PLC substrate. For these experiments I reconstituted the signaling cascade in Chinese hamster ovary (CHO) cells by transient over-expression of human TASK3 together with human muscarinic receptor 1 (M1R) and measured whole-cell TASK currents that were elicited by voltage ramps from -100 mV to +50 mV. Under these conditions, M1R stimulation by oxotremorine-M (Oxo-M) led to inhibition of TASK currents by approximately 80% at +50 mV in less than 20 s, which was reversible within minutes. All manipulations of PLC signaling were confirmed in control experiments using the DAG sensor GFP-PKCγ-C1[73] (Conserved-domain 1 of PKCγ, N-terminally fused to GFP) domain to report PLC activity. This GFP-PKCγ-C1 domain was monitored using total internal reflection (TIRF) microscopy. In this microscopy technique, laser light is completely reflected on the glass-sample interface and thus produces an evanescent field, which decays exponentially and can consequently only excite fluorophores in close proximity of approximately 100 nm to the glass bottom. The increase of plasma membrane DAG levels caused by PLC stimulation subsequently led to translocation of PKCγ-C1 to the membrane, which increased the fluorescence measured in TIRF.

In a first set of experiments I used the PLC inhibitor U73122, which had been previously employed to test whether functional PLC was necessary for receptor-mediated TASK channel inhibition, but with contradicting results[9,17,18,23,88]. To validate successful inhibition of PLC by U73122, I measured the translocation of the DAG probe GFP-PKCγ-C1. Under control conditions after pre-incubation with the inactive analog U73343, application of the M1R agonist Oxo-M caused a reversible increase in membrane association of PKCγ-C1, reflecting a strong DAG production (data not shown; Fig. 1d-f show similar control experiments performed by Dr. Moritz Lindner. He used the PIP_2- and IP_3-binding Pleckstrin-homology domain of PLCδ1, PLCδ1-PH[91], instead of the DAG sensor as a reporter for PLC activity.) In contrast, pre-incubation with U73122 impaired the rise of membrane association of the DAG probe, indicating effective PLC block in my experimental conditions. Analogously, TASK3 currents were inhibited upon M1R activation under

control (U73343) conditions, but were unaffected by M1R stimulation when PLC was blocked by pre-incubation with U73122 (Fig. 1a-c).

I further tested the PLC requirement with a molecular-biological approach to interfere with PLC signaling. To this end I used Gαq/11 knockout (Gαq/11 $^{-/-}$) cells[18] co-transfected with TASK3 or the DAG sensor GFP-PKCγ-C1, M1R and mutant Gαq proteins. A double mutation in Gαq (Gαq-AA) was previously suggested to render this G-protein incapable of PLC stimulation[18,101]. In a previous study, this mutant retained receptor-mediated TASK inhibition, which was taken to indicate that PLC was dispensable for regulation of TASK channels. However, when I tested this Gαq-AA mutant for its ability to activate PLC, PKCγ-C1 membrane translocation upon M1R stimulation revealed robust PLC activation (Fig. 1g, h). Even Gαq-5A, carrying additional mutations believed to interfere with PLC signaling[101], was still capable of stimulating PLC (Fig. 1g, h). Similarly, neither Gαq-AA nor Gαq-5A co-transfected in Gαq/11 $^{-/-}$ cells impaired TASK inhibition by receptor activation (Fig. 1i, j). The essential controls using the DAG sensor demonstrate that inhibition of TASK by Gαq-AA does not argue against an involvement of PLC in TASK signaling. In order to fully eliminate the signaling from activated Gαq to PLC, I used a recently developed chimera between Gαq and Gαi, termed Gαqiq[103]. Indeed, Gαqiq co-expression did not cause an increase in TIRF signal of PKCγ-C1 upon Oxo-M application, indicating that it failed to reconstitute the signaling cascade from M1R to PLC (Fig. 1g, h). In accordance, TASK3 inhibition by Oxo-M was lost by Gαqiq co-expression (Fig. 1i, j). These results are in line with the pharmacological data, suggesting that PLC activity is necessary for receptor-mediated TASK channel inhibition.

Calcium requirement of all PLC activity[38,39] enabled us to easily eliminate PLC signaling by calcium buffering of intracellular solution via dialysis through the patch pipette. Strong intracellular calcium buffering with 20 mM BAPTA completely blocked PKCγ-C1 membrane recruitment and TASK3 inhibition by M1R stimulation when recorded simultaneously (Fig. 2a, b). In contrast, weaker buffering with 5 mM BAPTA or 20 mM EGTA only attenuated receptor-mediated TASK inhibition (Fig. 2b). Because calcium dependence is a common property of many cellular processes, one might argue that signaling upstream of PLC is impaired in these experiments. Therefore I measured the interaction of activated Gαq-CFP and YFP-PLCβ3 induced by M1R stimulation by means of dynamic Förster resonance energy transfer (FRET). In this approach, an increase of FRET due to close association of the fluorophores of Gαq-CFP and YFP-PLCβ3 indicated effective signaling to activate PLC. The FRET increase under Oxo-M stimulation was essentially the same for control intracellular solution and 20 mM BAPTA, which demonstrates intact signaling to PLC in both conditions (Fig. 2c).

If PLC activity is required for signaling from GqPCRs to TASK channels, then this should depend on the availability of the PLC substrate PIP_2. To deplete PIP_2, I used the dual specificity 4'- and 5'-phosphatase pseudojanin introduced by Lindner *et al.* (2011)[55]. This chimera derived from yeast SAC and human INPP5E can be chemically recruited to the membrane by rapamycin to dephosphorylate phosphatidylinositol(4)phosphate (PIP) and PIP_2 at the 4'- and 5'-position, respectively[55] (Fig. 2d). Membrane recruitment of pseudojanin completely impaired subsequent

production of DAG in response to GqPCR activation as measured in TIRF experiments, in line with full depletion of the PLC substrate (Fig. 2e). In the corresponding electrophysiological experiment, TASK currents were not suppressed after M1R activation in cells depleted of PIP_2 (identified by cytoplasmic localization of the GFP-fused PIP_2 sensor PLCδ1-PH; Fig. 2f). Interestingly, in a previous study depletion of the PLC substrate PIP_2 by induction of a genetically encoded 5'-phosphatase was not sufficient to abolish receptor-mediated TASK inhibition[18]. In a parallel approach, I utilized the recruitment of a selective 5'-phosphatase activity (the SAC-mutant of pseudojanin) to acutely deplete PIP_2 avoiding changes in lipid metabolism that may occur due to long-time exposure of the cells to phosphatase activity. In line with Chen *et al.* (2006), I found robust receptor-mediated TASK inhibition despite PIP_2 depletion (Fig. 2f). Importantly, using the PKCγ-C1 DAG probe in TIRF experiments, I also revealed strong DAG production under these conditions (Fig. 2e), indicating that PLC downstream signaling is not impaired by activation of a 5'-PI phosphatase.

Finally, to test whether PLC activity is also sufficient for TASK inhibition, I used the membrane-permeable PLC activator m-3M3FBS to stimulate PLC[3,38]. PKCγ-C1 membrane translocation was robust upon application of 50 µM m-3M3FBS (Fig. 2g), but with slower kinetics and reduced amplitude when compared to the effects evoked by the M1R agonist Oxo-M, in line with previously reported effects of m-3M3FBS on PLC activity[3,38]. The compound evoked slow and reversible inhibition of TASK currents (Fig. 2h). In contrast, the inactive analog o-3M3FBS failed to affect plasma membrane DAG levels and caused only an insignificant TASK current reduction (Fig. 2g, h).

In summary, inhibition of PLC activity by either pharmacological block of the enzyme, interference with Gαq-coupling to PLC, buffering of an essential cofactor for PLC activity, or complete depletion of its substrate all eliminated GqPCR-mediated TASK inhibition. To conclude, these data clearly implicate a pivotal role for PLC in receptor-mediated TASK channel inhibition. Furthermore, activation of PLC seems sufficient to inhibit TASK currents, which suggests no major contribution of PLC-independent second messengers.

4.2 DAG is responsible for receptor-mediated TASK inhibition

Although TASK channel inhibition was caused by signaling events downstream of PLC, depletion of the PLC substrate PIP_2 (and potentially PIP) *per se* is not sufficient, as shown in Figure 2f and previously by Lindner *et al.*[55]. Thus, the hydrolysis products of PLC, DAG and IP_3, or IP_3-induced high intracellular calcium concentration remain as candidate messengers inhibiting TASK channels. Neither IP_3 itself nor calcium affected TASK currents in previous studies[17,23]. Therefore I examined the effect of DAG on whole-cell TASK currents by application of its membrane-permeable analog 1,2-dioctanoyl-sn-glycerol (DiC8). Both TASK1 and TASK3 were reversibly inhibited by 10 µM and 100 µM of this DAG analog in a dose-dependent manner (Fig. 3a, b). Application of DiC8 to CHO cells expressing PKCγ-C1 and M1R produced sub-maximal membrane translocation of the DAG probe, indicating that the achieved membrane concentrations of DAG are within physiological levels (Fig. 3c). Before the DAG-sensor translocated to the

plasma membrane upon DiC8 application, an unexpected initial decrease in membrane association of PKCγ-C1 was detected. This was probably caused by TIRF recording conditions, as it was absent in confocal imaging (Fig. 3c; confocal data not shown).

Next I aimed to substantiate the role of DAG for TASK channel inhibition during receptor activation by interfering in receptor-induced DAG transients. To this end I over-expressed a DAG-kinase (DGK) or DAG-lipase (DGL), which eliminate DAG by phosphorylation to PA and hydrolysis to 2-AG, respectively. The M1R-induced DAG increase measured by PKCγ-C1 was strongly attenuated when either the membrane-associated rat DGKβ or human DGLα were co-expressed with M1R (Fig. 5a-c). Accordingly, TASK3 current inhibition by Oxo-M application was blunted under co-expression of either DGK or DGL (Fig. 5d-f). This indicates that the DAG transients evoked by GqPCR stimulation are sufficient to evoke TASK channel inhibition. Furthermore, these results suggest no major role for the downstream metabolites PA and 2-AG, as their levels should be increased by co-expression of DGK and DGL, respectively.

4.3 Relevance of the 'VLRFLT' motif for channel inhibition by GqPCR and DAG

If DAG underlies GqPCR-mediated TASK inhibition, application of DiC8 should involve the same molecular mechanism of channel regulation as M1R stimulation. It has been shown previously that the six amino-acid motif 'VLRFLT' at the most proximal C-terminus is crucial for TASK3 inhibition by GqPCRs[98]. Therefore, I probed the role of this motif in DAG-induced TASK3 inhibition with C-terminally truncated TASK3 channels (Fig. 6a), in which the 'VLRFLT' motif was retained (Δ249) or deleted (Δ244). Both mutants gave rise to reduced current densities when expressed in CHO cells, but retained their sensitivity to extracellular acidification, indicating that the mutant channels were functional (Fig. 6b, c). Deletion of the C-terminus alone (Δ249, keeping the 'VLRFLT' motif intact) yielded channels still sensitive to inhibition by M1R stimulation and DiC8 application (Fig. 6b, c). However, both GqPCR activation and DiC8 application failed to inhibit TASK3 whole-cell currents when the 'VLRFLT' motif was also removed (Δ244; Fig. 6b, c). Similarly, the degree of TASK3 inhibition by DiC8 and receptor stimulation also correlated in channel mutants carrying single alanine mutations within this motif (Fig. 6d-f). For example, substitution of the positively charged arginine (R245A) or the branched leucine (L244A) strongly impaired both receptor-mediated inhibition and block by DiC8 (Fig. 6d-f). In contrast, channel regulation by Oxo-M and DiC8 was only partially attenuated when valine was mutated (V243A). These mutant studies confirm the critical involvement of the 'VLRFLT' motif for both GqPCR- and DAG-mediated TASK3 inhibition. The correlation of the strength of inhibition by M1R stimulation and DiC8 application is in line with the hypothesis that M1R causes channel inhibition by DAG.

4.4 Effect of DAG on the native TASK-mediated current IK_{SO} in CGNs

After identification of DAG as the responsible second messenger for GqPCR-mediated TASK channel inhibition in heterologous systems, I asked whether native TASK-mediated currents are also sensitive to DAG. Cerebellar granule neurons (CGNs) have been shown to express TASK1

and TASK3, which mediate the GqPCR- and pH-sensitive IK_{SO}[1,10,35,40,41,68]. To electrophysiologically measure these CGNs, I used dissociated CGNs from 6-9-day-old rats kept in culture in depolarizing high-potassium condition for 7-12 days to allow for outgrowth and development of IK_{SO}[35,44]. Whole-cell measurements of CGNs revealed an outwardly rectifying potassium conductance, IK_{SO}, known to be mediated by TASK[1,10]. IK_{SO} was blocked by extracellular acidification to pH 5.9 and was inhibited by application of 10 µM Oxo-M (Fig. 6a, b). Responses evoked by 100 µM DiC8 were similar, albeit with a slower kinetic, in agreement with the slow TASK inhibition found in heterologous systems by application of this lipid (Fig. 6a, b and compare to Fig. 3a-d). When DiC8 was applied on top of acidification, it had only a minor additional effect (Fig. 6c), suggesting that the DiC8-sensitive current is carried mainly by TASK channels, identified by their pH sensitivity. In agreement with the significant contribution of IK_{SO} to setting the membrane potential, inhibition of this conductance by DiC8 or Oxo-M evoked robust and highly significant depolarization (Fig. 7d, e). In summary, the inhibition of IK_{SO} by the DAG analog DiC8 strongly suggests that native TASK channels are also DAG-sensitive, consistent with a role of DAG in neuronal regulation of TASK similar to that found in our heterologous system.

5 Discussion

In my thesis I solved the underlying signaling mechanism responsible for TASK current reduction by GqPCRs, specifically that the second messenger DAG mediates TASK channel inhibition. As the main findings of this thesis, I emphasized the crucial role of PLC for the transmission of the signal from the receptor to the channel and demonstrated that the PLC-downstream signaling messenger DAG is sufficient to inhibit TASK1 and TASK3 channels.

5.1 PLC activity is both necessary and sufficient to inhibit TASK channels

The data I have presented provide substantial evidence that PLC activity is essential for receptor-mediated TASK inhibition and further offers explanations for previous discrepancies regarding the involvement of PLC[9,17,18,23,88]. When PLC signaling was disrupted through pre-application of the pharmacological inhibitor U73122, GqPCRs failed to inhibit TASK channels, in line with previous results[17,23,88]. However, these findings go against the work from Chen *et al.* (2006) and Boyd *et al.* (2000), who did not find an effect of U73122 on GqPCR-induced TASK channel inhibition, which might be explained by the instability of U73122 in aqueous solutions[9,18,45]. Additionally, Chen *et al.* (2006) used induction of a 5'-phosphatase to deplete the PLC substrate PIP_2, thereby disrupting PLC signaling[18]. In these experiments they still found GqPCR-evoked block of TASK activity, suggesting a PLC-independent mechanism for TASK inhibition[18]. While replicating their findings, control experiments in the present work showed robust DAG production despite pre-depletion of PIP_2 by a 5'-phosphatase (see Fig. 1g-j and Fig. 2d-f), contradicting the classical view of PLC-mediated PIP_2 hydrolysis as the elusive source of DAG. Rather, this observation can be explained in two ways, which both reveal an interesting aspect of PLC-DAG signaling: 1) PIP_2 concentration may not be reduced to zero by the experimentally induced 5'-phosphatase activity, because of rapid, compensatory PIP_2 re-synthesis. Thus, PIP_2 levels under these conditions may be too low for most PIP_2 effectors to maintain PIP_2 binding, but sufficient to allow for generation of DAG and IP_3/calcium. 2) Alternatively, PIP_2 may be essentially depleted to zero in my experimental conditions. Because plasma membrane levels of phosphoinositides other than PIP and PIP_2 are low, the detected DAG increase can only result from hydrolysis of PIP by PLC, yielding DAG and IP_2 rather than IP_3 (as from PIP_2 cleavage). In this scenario, DAG transients evoked by PLC should occur without a rise of intracellular calcium and independently of the availability of PIP_2. Support both for fast PIP_2 re-synthesis[26,31], as well as for hydrolysis of PIP by PLC[38,52] can be found in the literature. Taken together, PLC activity is required for TASK channel inhibition by membrane receptors, but detectable PIP_2 levels may not be necessary for significant downstream PLC signaling. These findings have considerable implications for our understanding of cell signaling: Firstly, it could allow for sustained DAG production by PLC signaling despite profound PIP_2 depletion in the plasma membrane. Secondly, PLC (for example activated by high calcium) can cause DAG increase in intracellular compartments, where PIP_2 is low or absent[74,91]. It is exciting to speculate, whether this could affect the third member of the TASK channel family, TASK5. It is expressed in the auditory pathway, but no plasma-membrane conductance was assigned to this channel so far[41,42]. With intracellu-

lar potassium channels coming more in the focus of research[16], it may be interesting to investigate intracellular TASK5 activity and its possible regulation by PLC.

5.2 DAG mediates TASK channel inhibition by GqPCRs

I found by means of over-expression of the DAG-metabolizing enzymes DGK and DGL that DAG is the responsible second messenger downstream of PLC for TASK inhibition. Since these enzymes attenuated both DAG transients and TASK current inhibition during GqPCR activation, these data precluded an involvement of DAG metabolites in TASK3 inhibition, because PA and 2-AG should be increased upon expression of DGKβ and DGLα, respectively. This conclusion was additionally supported by results from excised macropatches (*Xenopus* oocytes) obtained by Dr. Moritz Lindner presented in figure 4a and b. These data showed no effect of PA or AA (which can result by further hydrolysis of DAG or 2-monoacylglycerol at the sn2-postition) on TASK3. In contrast, application of 20 μM 2-AG on excised patches showed approximately 50% inhibition (see Fig. 4a, b). However, whether or not this lipid is physiologically relevant during GqPCR signaling will be determined by the concentration it reaches, which depends on the expression of the different DGL and DGK isoforms, their respective activity as well as the downstream 2-AG metabolism.

The data from the overexpression experiments of DGK and DGL demonstrate that the physiological plasma membrane concentrations of native DAG species reached upon GqPCR activation mediate inhibition of TASK channels. However, many pharmacological and biochemical aspects of TASK channel block by DAG remain speculative. Because quantification of DAG levels in the membrane during receptor stimulation or direct application of DAG analogs is difficult, obtaining an exact dose response curve is challenging. However, the IC_{50} value of 10 μM obtained for SAG applied on excised patches can serve as good approximation (see figure 4f, data from Dr. Moritz Lindner). Another remaining question about TASK channel inhibition is the impact of the fatty acid composition of the DAG species involved. Although detailed investigations remain necessary, there is already some indication that the lipid moiety in DAG does affect channel inhibition: The DAG analog 1-oleoyl-2-acetyl-sn-glycerol composed of a long, monounsaturated fatty acid chain and the short acetyl group has a reduced efficiency to inhibit TASK channels (400 μM caused 30% inhibition of whole-cell TASK currents, unpublished results). Taken together, the influence of the lipid composition of DAG on the efficiency of TASK channel inhibition remains to be fully elucidated.

5.3 DAG probably inhibits TASK channels directly

DAG could impart its inhibiting effect on TASK channels either by directly affecting TASK activity or by additional downstream signaling, like the DAG effector PKC. Indeed, it is known that PKC can phosphorylate the TASK C-terminus, thereby reducing TASK whole-cell currents[58,100]. However, this mechanism does not seem to mediate channel inhibition by GqPCRs, because neither application of a PKC inhibitor nor mutations of the PKC consensus sites in the channel abolished receptor-induced TASK regulation[17,23,88,100]. My data substantiate a

PKC-independent mechanism of channel inhibition by two lines of evidence: Firstly, the C-terminally truncated channels retained DAG- and GqPCR-mediated TASK inhibition (see Fig. 6b, c), although it had been shown previously that this truncated channel lost inhibition by PKC[100]. Secondly, DAG analogs inhibited TASK currents in inside-out macropatches, where cytoplasmic proteins are not preserved (see Fig. 3d-f).

Next, it is worth considering whether DAG acts through an accessory protein, or whether it binds directly to TASK channels. Although the proteins 14-3-3, p11, COP1, and NOX4 have been shown to bind TASK channels and regulate intracellular trafficking or oxygen sensitivity, no role in GqPCR-mediated channel inhibition of these proteins has been reported so far[65]. Thus, there is no known candidate accessory protein to mediate the DAG effect. Furthermore, I found DAG sensitivity of TASK channels in neurons, CHO cells and oocytes, and GqPCR-meditated inhibition of TASK currents has been shown in a plethora of cell types, indicating that if a potential accessory protein confers DAG sensitivity it would have to be ubiquitously expressed. In addition, truncation of the C-terminus (Δ249, Fig 6) left only a short 'core channel' with little intracellular portion remaining (seven amino acids N-terminally and approximately 30 amino acids as the TMD2-TMD3 linker), thus potential protein interaction sites are largely eliminated without affecting DAG sensitivity. In conclusion, involvement of an additional protein to confer the DAG response to TASK channel seems unlikely, indicating direct binding of DAG as the most probable mechanism.

5.4 Role of the 'VLRFLT' motif: gate or DAG binding site?

Shortly after identification of TASK channels, a six-amino-acid motif (VLRFMT in TASK1, VLRFLT in TASK3) was found to mediate the response to volatile anesthetics as well as the inhibition by GqPCRs[76,98]. Later it was recognized that the same region was also crucial for direct TASK1 channel inhibition by the endocannabinoid anandamide[99]. Using TASK1/3 concatamers, Talley and Bayliss (2002) found that disruption of this site in only one subunit already abrogated the regulation by GqPCRs and halothane[98]. Sequence alignment with other members of the K2P channel family and comparison of the respective crystal structures does not allow for an unambiguous localization of this motif within the channel structure, but it is likely part of the distal TMD4 helix[12,27,70]. From my results using mutant channels I conclude that this 'VLRFLT' motif is essential for TASK current inhibition by DAG, but these findings also raise the next issue: Is this motif a DAG binding site, or is it a critical gating element?

With DAG being a membrane-resident second messenger with a polar head group, potential DAG binding sites in TASK channels would need to be closely associated with the membrane or even partially inserted into it. The 'VLRFL/MT' motif positioned at the interface between the plasma membrane and the cytosol meets this requirement for DAG sensing. Interestingly, in their X-ray crystal structure Dong *et al.* (2015) found a lipid-like density bound between TMD4 and TMD3 in the non-conductive TREK2 down state (this density was absent in the conductive state)[27]. Mutations in TMD4 of amino acids (M322A, W326A) directed towards the TMD3-TMD4 interface reduced TREK2 channel activation by membrane stretch[27]. The mutation W326A in

TREK2 is homologous to the TASK3 mutation R245A, which abolished GqPCR- and DAG-mediated channel inhibition in my work. Furthermore, mutations at very similar positions of TMD3 in both channels, R237A in TREK2 and M157W in TASK3, impair channel regulation by membrane stretch and GqPCRs, respectively[21,27]. Thus, an interaction with these amino acids, possibly by DAG binding between the TMD3 and TMD4 of TASK channels, might cause channel transition to a non-conductive state. This idea is particularly attractive since the C-terminally truncated TASK channel (Δ249 in figure 6, comprising of a short, seven-amino-acid intracellular N-terminus and approximately 30-amino-acid TMD2-TMD3 linker, see Fig 6) is also inhibited by DAG. Therefore, potential DAG binding sites are restricted to the cytosolic facing part of this minimalistic channel, making the 'VLRFLT' motif a reasonable candidate for the site of DAG regulation.

In contrast to the previously discussed mechanism of DAG binding to the 'VLRFLT' motif, the importance of this amino acid stretch may also be explained with its role in channel gating. The gate of K2P channels has been suggested to be associated with the selectivity filter[78,87]. A connection between the postulated gate at the filter and the C-terminal 'VLRFLT' motif can be drawn by the solved TREK2 structures[27]. Comparison of the up-state with the non-conductive down-state revealed a notable flexion and rotation of the TMD4 at the hinge glycine, involving changes in the TMD3-TMD4 interaction[27]. Assuming a similar gating mechanism within the K2P channel family, this movement of TMD4 could require an intact 'VLRFLT' motif for TASK channel gating by DAG. However, how DAG initiates the regulatory signal to gate TASK channels in this model would remain elusive, but cannot involve the channel's C-terminus, since inhibition by DAG is maintained despite C-terminal truncation of the channel.

Similar to inhibition by DAG, it has been shown that TASK channel regulation by other compounds, e.g. the volatile anesthetic halothane and an analog of the endocannabinoid anandamide, also depends on the integrity of the VLRFL/MT motif[76,98,99]. Whether these different substances share the same binding site on TASK, or rather the same gating mode, requires further investigation.

5.5 Implications of my findings and outlook

While cell signaling is often described as distinct hierarchic signaling 'pathways', it becomes clear that it is rather a complex network with divergent and convergent flows of information[63,77]. Thus, knowledge of the precise second messenger involved in protein regulation is required in order to estimate the impact of cross-talk between the classical signaling cascades. For example, activation of over-expressed PLCβ2 by Gβγ subunits released in Gαi signaling is sufficient to inhibit TASK currents[23]. In addition to that, the temporal and spacial signaling patterns are unique for each second messenger and strongly influences signaling output[72]. For TASK channel inhibition by DAG, this regulation may depend on the spacial arrangement of receptors, PLC and its substrates, DAG metabolizing enzymes, and TASK channels. The localization of the involved lipids and proteins can be regulated by scaffolding proteins to form signaling complexes, which may explain the co-immunoprecipitation of activated Gαq with TASK channels[18]. In addi-

tion to regulation of DAG levels within the plasma membrane, intracellular compartments can also affect plasma membrane DAG *in trans* at specific contact sites with the endoplasmic reticulum[86].

Considering the results from the perspective of DAG signaling, TASK adds a potassium channel to the known DAG effectors TRPC2/3/6/7 and proteins which contain a C1-domain [14,37,60]. Classically, DAG-mediated signaling depends on C1 domains, first identified in PKC and subsequently found in many protein and lipid kinases, small G-protein interacting proteins, and scaffolds[24]. These proteins translocate to the membrane upon binding of DAG to their C1 domains and this subsequently induces activation. The crystal structure of these 50/51 amino acids containing C1 domains as well as the mechanism of DAG binding and membrane recruitment is well known[24]. In contrast to C1-mediated DAG signaling, the mechanism of activation of TRPC channels by DAG has not been elucidated so far. The size of TRPC proteins und TRPC regulation by multiple modulators complicates the study on DAG-induced TRPC activation. Inhibition of the truncated TASK3 channel by DAG, the known importance of the 'VLRFLT' amino acid stretch at the proximal C-terminus, and the possibility of TASK channel modeling based on several known K2P crystal structures provide the chance to elucidate the DAG-binding mechanism to ion channels and may allow for transfer of this knowledge to unravel TRPC regulation by DAG.

Taken together, the knowledge of the inhibition of TASK channels by DAG does not only provide the basis for studying the interesting mechanistic aspect of DAG effects on ion channels. Most importantly, it expands our understanding of the roles of DAG by linking DAG levels to the electrophysiological properties of cells. Thus, the DAG transients evoked by PLC stimulation upon GqPCR activation underlies TASK1 and TASK3 channel inhibition. In conclusion, the influence of TASK channel activity on the membrane potential depends on DAG dynamics, affecting pivotal cellular functions such as action potential formation and hormone secretion.

6 List of abbreviations

AA	Arachidonic acid
CGN	Cerebellar granule cells
C1	Conserved region 1
DAG	1,2-Diacylglycerol
DiC8	1,2-Dioctanoyl-sn-glycerol, a membrane-permeable DAG analog
FRET	Förster resonance energy transfer
Gαq	αq-subunit of heterotrimeric G-proteins
Gαqiq	chimera of αq- and αi- subunit of heterotrimeric G-proteins
GDP	Guanosin diphosphate
GFP	Green fluorescent protein
GqPCR	Gq-protein coupled receptor
GRK	GPCR kinases
GTP	Guanosin triphosphate
IK_{SO}	Standing outward potassium current
IP_2	Inositol(1,4)bisphosphate
IP_3	Inositol(1,4,5)trisphophate
K2P	Two-pore potassium channel
M1R	Muscarinic receptor 1
Oxo-M	Oxotremorine-M (muscarinic receptor agonist)
PA	Phosphatidic acid
PH	Pleckstrin homology
PIP	Phosphatidylinositol(4)phosphate
PIP_2	Phosphatidylinositol(4,5)bisphosphate
PIP_3	Phosphatidylinositol(3,4,5)trisphosphate
PKC	Proteinkinase C
PKCγ-C1	C1 domain derived from proteinkinase C; DAG probe
PLCβ	Phospholipase Cβ
PLCδ1-PH	PH domain from phospholipase Cδ1; PIP and PIP_2 binding probe
TALK	TWIK-related alkaline pH activated potassium channel
TASK	TWIK-related acid sensitive potassium channel
THIK	Tandem-pore domain halothane inhibited potassium channel
TIRF	Total internal reflection fluorescence
TMD	Transmembrane domain
TRAAK	TWIK-related arachidonic acid stimulated potassium channel
TREK	TWIK-related potassium channel
TRESK	TWIK-related spinal cord potassium channel
TWIK	Tandem of P domains in weak inward rectifier potassium channel
2-AG	2-Arachidonoylglycerol

7 References

1. Aller, M. I. *et al.* Modifying the subunit composition of TASK channels alters the modulation of a leak conductance in cerebellar granule neurons. *J. Neurosci.* 25, 11455–67 (2005).
2. Ashmole, I. *et al.* The response of the tandem pore potassium channel TASK-3 (K(2P)9.1) to voltage: gating at the cytoplasmic mouth. *J. Physiol.* 587, 4769–83 (2009).
3. Bae, Y.-S. *et al.* Identification of a compound that directly stimulates phospholipase C activity. *Mol. Pharmacol.* 63, 1043–50 (2003).
4. Bandulik, S., Tauber, P., Lalli, E., Barhanin, J. & Warth, R. Two-pore domain potassium channels in the adrenal cortex. *Pflugers Arch. Eur. J. Physiol.* 1027–1042 (2014). doi:10.1007/s00424-014-1628-6
5. Ben-Abu, Y., Zhou, Y., Zilberberg, N. & Yifrach, O. Inverse coupling in leak and voltage-activated K+ channel gates underlies distinct roles in electrical signaling. *Nat. Struct. Mol. Biol.* 16, 71–79 (2009).
6. Berg, A. P. Motoneurons Express Heteromeric TWIK-Related Acid-Sensitive K+ (TASK) Channels Containing TASK-1 (KCNK3) and TASK-3 (KCNK9) Subunits. *J. Neurosci.* 24, 6693–6702 (2004).
7. Black, J. B., Premont, R. T. & Daaka, Y. Feedback Regulation of G Protein-Coupled Receptor Signaling by GRKs and Arrestins. *Semin. Cell Dev. Biol.* 50, 95–104 (2016).
8. Blin, S. *et al.* Mixing and matching TREK/TRAAK subunits generate heterodimeric K_{2P} channels with unique properties. *Proc. Natl. Acad. Sci.* 113, 201522748 (2016).
9. Boyd, D. F., Millar, J. A., Watkins, C. S. & Mathie, A. The role of Ca2+ stores in the muscarinic inhibition of the K+ current IK(SO) in neonatal rat cerebellar granule cells. *J. Physiol.* 529 Pt 2, 321–31 (2000).
10. Brickley, S. G. *et al.* TASK-3 two-pore domain potassium channels enable sustained high-frequency firing in cerebellar granule neurons. *J. Neurosci.* 27, 9329–40 (2007).
11. Brohawn, S. G., del Marmol, J., MacKinnon, R., del Mármol, J. & MacKinnon, R. Crystal structure of the human K2P TRAAK, a lipid- and mechano-sensitive K+ ion channel.-SOM. *Science (80-.).* 335, 436–441 (2012).
12. Brohawn, S. G., Campbell, E. B. & MacKinnon, R. Domain-swapped chain connectivity and gated membrane access in a Fab-mediated crystal of the human TRAAK K+ channel. *Proc. Natl. Acad. Sci. U. S. A.* 110, 2129–34 (2013).
13. Brose, N., Betz, A. & Wegmeyer, H. Divergent and convergent signaling by the diacylglycerol second messenger pathway in mammals. *Curr. Opin. Neurobiol.* 14, 328–40 (2004).
14. Carrasco, S. & Mérida, I. Diacylglycerol, when simplicity becomes complex. *Trends Biochem. Sci.* 32, 27–36 (2007).
15. Chapman, C. G. *et al.* Cloning, localisation and functional expression of a novel human, cerebellum specific, two pore domain potassium channel. *Brain Res. Mol. Brain Res.* 82, 74–83 (2000).
16. Checchetto, V., Teardo, E., Carraretto, L., Leanza, L. & Szabo, I. Physiology of intracellular potassium channels: a unifying role as mediators of counterion fluxes? *Biochim. Biophys. Acta - Bioenerg.* 1857, 1258–1266 (2016).
17. Chemin, J. *et al.* Mechanisms underlying excitatory effects of group I metabotropic glutamate receptors via inhibition of 2P domain K+ channels. *EMBO J.* 22, 5403–11 (2003).
18. Chen, X. *et al.* Inhibition of a background potassium channel by Gq protein alpha-subunits. *Proc. Natl. Acad. Sci. U. S. A.* 103, 3422–7 (2006).
19. Clarke, C. E., Veale, E. L., Green, P. J., Meadows, H. J. & Mathie, A. Selective block of the human 2-P domain potassium channel, TASK-3, and the native leak potassium current, IKSO, by zinc. *J. Physiol.* 560, 51–62 (2004).
20. Cohen, A., Ben-Abu, Y. & Zilberberg, N. Gating the pore of potassium leak channels. *Eur. Biophys. J.* 39, 61–73 (2009).

21. Conway, K. E. & Cotten, J. F. Covalent modification of a volatile anesthetic regulatory site activates TASK-3 (KCNK9) tandem-pore potassium channels. *Mol. Pharmacol.* 81, 393–400 (2012).

22. Czirják, G. & Enyedi, P. Formation of functional heterodimers between the TASK-1 and TASK-3 two-pore domain potassium channel subunits. *J. Biol. Chem.* 277, 5426–5432 (2002).

23. Czirják, G., Petheo, G. L., Spät, A. & Enyedi, P. Inhibition of TASK-1 potassium channel by phospholipase C. *Am. J. Physiol. Cell Physiol.* 281, C700-8 (2001).

24. Das, J. & Rahman, G. M. C1 domains: Structure and ligand-binding properties. *Chem. Rev.* 114, 12108–12131 (2014).

25. Díaz, W. G. *et al.* Insight into the Mechanism of pH Sensitivity in K 2P channel TASK3 from Molecular Dynamics Simulations. 47, 11100373 (2008).

26. Dickson, E. J., Falkenburger, B. H. & Hille, B. Quantitative properties and receptor reserve of the IP3 and calcium branch of Gq-coupled receptor signaling. *J. Gen. Physiol.* 141, 521–35 (2013).

27. Dong, Y. Y. *et al.* K2P channel gating mechanisms revealed by structures of TREK-2 and a complex with Prozac. *Science* 347, 1256–9 (2015).

28. Duprat, F. *et al.* TASK, a human background K+ channel to sense external pH variations near physiological pH. *EMBO J.* 16, 5464–71 (1997).

29. Eichmann, T. O. & Lass, A. DAG tales: the multiple faces of diacylglycerol–stereochemistry, metabolism, and signaling. *Cell. Mol. Life Sci.* (2015). doi:10.1007/s00018-015-1982-3

30. Enyedi, P. & Czirják, G. Molecular background of leak K+ currents: two-pore domain potassium channels. *Physiol. Rev.* 90, 559–605 (2010).

31. Falkenburger, B. H., Dickson, E. J. & Hille, B. Quantitative properties and receptor reserve of the DAG and PKC branch of G(q)-coupled receptor signaling. *J. Gen. Physiol.* 141, 537–55 (2013).

32. Goldstein, M. *et al.* Functional mutagenesis screens reveal the 'cap structure' formation in disulfide-bridge free TASK channels. *Sci. Rep.* 6, 19492 (2016).

33. Goldstein, S. A. N., Price, L. A., Rosenthal, D. N. & Pausch, M. H. ORK1, a potassium selective leak channel with wo pore domains cloned from Drosophila melanogaster by expression in Saccharomyces cerevisiae. *Pnas* 93, 13256–13261 (1996).

34. González, W. *et al.* An extracellular ion pathway plays a central role in the cooperative gating of a K2P K+ channel by extracellular pH. *J. Biol. Chem.* 288, 5984–5991 (2013).

35. Han, J., Truell, J., Gnatenco, C. & Kim, D. Characterization of four types of background potassium channels in rat cerebellar granule neurons. *J. Physiol.* 542, 431–444 (2002).

36. Hille, B. *Ion Channels of Excitable Membranes*. (Sinauer Associates, Inc., 2001).

37. Hofmann, T. *et al.* Direct activation of human TRPC6 and TRPC3 channels by diacylglycerol. *Nature* 397, 259–63 (1999).

38. Horowitz, L. F. *et al.* Phospholipase C in living cells: activation, inhibition, Ca2+ requirement, and regulation of M current. *J. Gen. Physiol.* 126, 243–62 (2005).

39. Kadamur, G. & Ross, E. M. Mammalian phospholipase C. *Annu Rev Physiol* 75, 127–154 (2013).

40. Kang, D., Han, J., Talley, E. M., Bayliss, D. a & Kim, D. Functional expression of TASK-1/TASK-3 heteromers in cerebellar granule cells. *J. Physiol.* 554, 64–77 (2004).

41. Karschin, C. *et al.* Expression pattern in brain of TASK-1, TASK-3, and a tandem pore domain K(+) channel subunit, TASK-5, associated with the central auditory nervous system. *Mol. Cell. Neurosci.* 18, 632–48 (2001).

42. Kim, D. & Gnatenco, C. TASK-5, a new member of the tandem-pore K(+) channel family. *Biochem. Biophys. Res. Commun.* 284, 923–930 (2001).

43. Kim, Y., Bang, H. & Kim, D. TASK-3, a new member of the tandem pore K(+) channel family. *J. Biol. Chem.* 275, 9340–7 (2000).

44. Lauritzen, I. *et al.* K+-dependent cerebellar granule neuron apoptosis. Role of task leak K+ channels. *J. Biol. Chem.* 278, 32068–76 (2003).

45. Leitner, M. G. *et al.* Direct modulation of TRPM4 and TRPM3 channels by the phospholipase C

inhibitor U73122. *Br. J. Pharmacol.* 2555–2569 (2016). doi:10.1111/bph.13538

46. Lengyel, M., Czirják, G. & Enyedi, P. Formation of Functional Heterodimers by TREK-1 and TREK-2 Two-pore Domain Potassium Channel Subunits. *J. Biol. Chem.* jbc.M116.719039 (2016). doi:10.1074/jbc.M116.719039

47. Leonoudakis, D. *et al.* An open rectifier potassium channel with two pore domains in tandem cloned from rat cerebellum. *J. Neurosci.* 18, 868–77 (1998).

48. Lesage, F. *et al.* Dimerization of TWIK-1 K+channel subunits via a disulfide bridge. *Embo J.* 15, 6400–6407 (1996).

49. Lesage, F. *et al.* TWIK-1, a ubiquitous human weakly inward rectifying K+ channel with a novel structure. *EMBO J.* 15, 1004–11 (1996).

50. Lesage, F. & Barhanin, J. Molecular physiology of pH-sensitive background K(2P) channels. *Physiology (Bethesda).* 26, 424–37 (2011).

51. Levitz, J. *et al.* Heterodimerization within the TREK channel subfamily produces a diverse family of highly regulated potassium channels. *Proc. Natl. Acad. Sci.* 113, 201522459 (2016).

52. Li, Y., Gamper, N., Hilgemann, D. W. & Shapiro, M. S. Regulation of Kv7 (KCNQ) K+ channel open probability by phosphatidylinositol 4,5-bisphosphate. *J. Neurosci.* 25, 9825–35 (2005).

53. Linden, A.-M. The in Vivo Contributions of TASK-1-Containing Channels to the Actions of Inhalation Anesthetics, the 2 Adrenergic Sedative Dexmedetomidine, and Cannabinoid Agonists. *J. Pharmacol. Exp. Ther.* 317, 615–626 (2006).

54. Linden, A.-M. *et al.* TASK-3 knockout mice exhibit exaggerated nocturnal activity, impairments in cognitive functions, and reduced sensitivity to inhalation anesthetics. *J. Pharmacol. Exp. Ther.* 323, 924–34 (2007).

55. Lindner, M., Leitner, M. G., Halaszovich, C. R., Hammond, G. R. V & Oliver, D. Probing the regulation of TASK potassium channels by PI(4,5)P_2 with switchable phosphoinositide phosphatases. *J. Physiol.* 589, 3149–62 (2011).

56. Litosch, I. Decoding Gαq signaling. *Life Sci.* 152, 99–106 (2016).

57. Lopes, C. M. B. *et al.* PIP2 hydrolysis underlies agonist-induced inhibition and regulates voltage gating of two-pore domain K+ channels. *J. Physiol.* 564, 117–29 (2005).

58. Lopes, C. M. B., Gallagher, P. G., Buck, M. E., Butler, M. H. & Goldstein, S. A. N. Proton block and voltage gating are potassium-dependent in the cardiac leak channel Kcnk3. *J. Biol. Chem.* 275, 16969–16978 (2000).

59. Lotshaw, D. P. Biophysical, pharmacological, and functional characteristics of cloned and native mammalian two-pore domain K+ channels. *Cell Biochem. Biophys.* 47, 209–256 (2007).

60. Lucas, P., Ukhanov, K., Leinders-Zufall, T. & Zufall, F. A diacylglycerol-gated cation channel in vomeronasal neuron dendrites is impaired in TRPC2 mutant mice: mechanism of pheromone transduction. *Neuron* 40, 551–61 (2003).

61. Lutz, S. *et al.* The guanine nucleotide exchange factor p63RhoGEF, a specific link between Gq/11-coupled receptor signaling and RhoA. *J. Biol. Chem.* 280, 11134–11139 (2005).

62. MacKenzie, G., Franks, N. P. & Brickley, S. G. Two-pore domain potassium channels enable action potential generation in the absence of voltage-gated potassium channels. *Pflugers Arch. Eur. J. Physiol.* 989–999 (2014). doi:10.1007/s00424-014-1660-6

63. Masuho, I. *et al.* Distinct profiles of functional discrimination among G proteins determine the actions of G protein–coupled receptors. *Sci. Signal.* 8, ra123-ra123 (2015).

64. Mathie, A. Neuronal two-pore-domain potassium channels and their regulation by G protein-coupled receptors. *J. Physiol.* 578, 377–85 (2007).

65. Mathie, A., Rees, K. A., Hachmane, M. F. El & Veale, E. L. Trafficking of Neuronal Two Pore Domain Potassium Channels. 276–286 (2010).

66. McCudden, C. R., Hains, M. D., Kimple, R. J., Siderovski, D. P. & Willard, F. S. G-protein signaling: back to the future. *Cell. Mol. Life Sci.* 62, 551–77 (2005).

67. Meuth, S. G. *et al.* Contribution of TWIK-related acid-sensitive K+ channel 1 (TASK1) and TASK3 channels to the control of activity modes in thalamocortical neurons. *J. Neurosci.* 23, 6460–

6469 (2003).

68. Millar, J. a *et al.* A functional role for the two-pore domain potassium channel TASK-1 in cerebellar granule neurons. *Proc. Natl. Acad. Sci. U. S. A.* 97, 3614–8 (2000).

69. Miller, A. & Long, S. Crystal Structure of the Human Two – Pore Domain Potassium Channel K2P1. *Science (80-.).* 335, 432 (2012).

70. Miller, A. N. & Long, S. B. Crystal structure of the human two-pore domain potassium channel K2P1.-SOM. *Science* 335, 432–6 (2012).

71. Musset, B. *et al.* Effects of divalent cations and spermine on the K+ channel TASK-3 and on the outward current in thalamic neurons. *J. Physiol.* 572, 639–57 (2006).

72. Oancea, E. & Meyer, T. Protein kinase C as a molecular machine for decoding calcium and diacylglycerol signals. *Cell* 95, 307–18 (1998).

73. Oancea, E., Teruel, M. N., Quest, a F. & Meyer, T. Green fluorescent protein (GFP)-tagged cysteine-rich domains from protein kinase C as fluorescent indicators for diacylglycerol signaling in living cells. *J. Cell Biol.* 140, 485–98 (1998).

74. Ozato-sakurai, N., Fujita, A. & Fujimoto, T. The Distribution of Phosphatidylinositol 4 , 5-Bisphosphate in Acinar Cells of Rat Pancreas Revealed with the Freeze-Fracture Replica Labeling Method. 6, (2011).

75. Di Paolo, G. & De Camilli, P. Phosphoinositides in cell regulation and membrane dynamics. *Nature* 443, 651–7 (2006).

76. Patel, a J. *et al.* Inhalational anesthetics activate two-pore-domain background K+ channels. *Nat. Neurosci.* 2, 422–6 (1999).

77. Philip, F., Kadamur, G., Silos, R. G., Woodson, J. & Ross, E. M. Synergistic activation of phospholipase C-beta3 by Galpha(q) and Gbetagamma describes a simple two-state coincidence detector. *Curr. Biol.* 20, 1327–35 (2010).

78. Piechotta, P. L. *et al.* The pore structure and gating mechanism of K2P channels. *EMBO J.* 30, 3607–19 (2011).

79. Plant, L. D., Zuniga, L., Araki, D., Marks, J. D. & Goldstein, S. a N. SUMOylation silences heterodimeric TASK potassium channels containing K2P1 subunits in cerebellar granule neurons. *Sci. Signal.* 5, ra84 (2012).

80. Putzke, C. *et al.* The acid-sensitive potassium channel TASK-1 in rat cardiac muscle. *Cardiovasc. Res.* 75, 59–68 (2007).

81. Rajan, S. *et al.* TASK-3, a novel tandem pore domain acid-sensitive K+ channel. An extracellular histiding as pH sensor. *J. Biol. Chem.* 275, 16650–7 (2000).

82. Renigunta, V., Schlichthörl, G. & Daut, J. Much more than a leak: structure and function of K2P-channels. *Pflugers Arch. Eur. J. Physiol.* 867–894 (2015). doi:10.1007/s00424-015-1703-7

83. Rhee, S. G. Regulation of phosphoinositide-specific phospholipase C. *Annu. Rev. Biochem.* 70, 281–312 (2001).

84. Rinné, S. *et al.* TASK-1 and TASK-3 may form heterodimers in human atrial cardiomyocytes. *J. Mol. Cell. Cardiol.* 81, 71–80 (2015).

85. Rjasanow, A., Leitner, M. G., Thallmair, V., Halaszovich, C. R. & Oliver, D. Ion channel regulation by phosphoinositides analyzed with VSPs-PI(4,5)P2 affinity, phosphoinositide selectivity, and PI(4,5)P2 pool accessibility. *Front. Pharmacol.* 6, 127 (2015).

86. Saheki, Y. *et al.* Control of plasma membrane lipid homeostasis by the extended synaptotagmins. 18, (2016).

87. Schewe, M. *et al.* A Non-canonical Voltage-Sensing Mechanism Controls Gating in K2P K+ Channels. *Cell* 164, 937–949 (2016).

88. Schiekel, J. *et al.* The inhibition of the potassium channel TASK-1 in rat cardiac muscle by endothelin-1 is mediated by phospholipase C. *Cardiovasc. Res.* 97, 97–105 (2013).

89. Seyler, C. *et al.* TASK1 (K(2P)3.1) K(+) channel inhibition by endothelin-1 is mediated through Rho kinase-dependent phosphorylation. *Br. J. Pharmacol.* 165, 1467–75 (2012).

90. Sirois, J. E., Lei, Q., Talley, E. M., Lynch, C. & Bayliss, D. a. The TASK-1 two-pore domain K+ channel is a molecular substrate for neuronal effects of inhalation anesthetics. *J. Neurosci.* 20, 6347–6354 (2000).

91. Stauffer, T. P., Ahn, S. & Meyer, T. Receptor-induced transient reduction in plasma membrane PtdIns(4,5)P2 concentration monitored in living cells. *Curr Biol* 8, 343–346 (1998).

92. Storch, U. *et al.* Dynamic NHERF interaction with TRPC4/5 proteins is required for channel gating by diacylglycerol. *Proc. Natl. Acad. Sci.* 201612263 (2016). doi:10.1073/pnas.1612263114

93. Streb, H., Irvine, R. F., Berridge, M. J. & Schulz, I. Release of Ca2+ from a nonmitochondrial intracellular store in pancreatic acinar cells by inositol-1,4,5-trisphosphate. *Nature* 306, 67–69 (1983).

94. Suh, B.-C. & Hille, B. Regulation of ion channels by phosphatidylinositol 4,5-bisphosphate. *Curr. Opin. Neurobiol.* 15, 370–8 (2005).

95. Suh, B.-C., Inoue, T., Meyer, T. & Hille, B. Rapid chemically induced changes of PtdIns(4,5)P2 gate KCNQ ion channels. *Science* 314, 1454–7 (2006).

96. Talley, E. M., Lei, Q., Sirois, J. E. & Bayliss, D. a. TASK-1, a two-pore domain K+ channel, is modulated by multiple neurotransmitters in motoneurons. *Neuron* 25, 399–410 (2000).

97. Talley, E. M., Solorzano, G., Lei, Q., Kim, D. & Bayliss, D. a. Cns distribution of members of the two-pore-domain (KCNK) potassium channel family. *J. Neurosci.* 21, 7491–7505 (2001).

98. Talley, E. M. & Bayliss, D. a. Modulation of TASK-1 (Kcnk3) and TASK-3 (Kcnk9) potassium channels: volatile anesthetics and neurotransmitters share a molecular site of action. *J. Biol. Chem.* 277, 17733–42 (2002).

99. Veale, E. L., Buswell, R., Clarke, C. E. & Mathie, A. Identification of a region in the TASK3 two pore domain potassium channel that is critical for its blockade by methanandamide. *Br. J. Pharmacol.* 152, 778–86 (2007).

100. Veale, E. L. *et al.* G(alpha)q-mediated regulation of TASK3 two-pore domain potassium channels: the role of protein kinase C. *Mol. Pharmacol.* 71, 1666–75 (2007).

101. Venkatakrishnan, G. & Exton, J. H. Identification of determinants in the alpha-subunit of Gq required for phospholipase C activation. *J. Biol. Chem.* 271, 5066–72 (1996).

102. Watkins, C. S. & Mathie, A. A non-inactivating K+ current sensitive to muscarinic receptor activation in rat cultured cerebellar granule neurons. *J. Physiol.* 491 (Pt 2, 401–12 (1996).

103. Zhang, X. *et al.* Direct inhibition of the cold-activated TRPM8 ion channel by Gα(q). *Nat. Cell Biol.* 14, 850–858 (2012).

104. Zilberberg, N., Ilan, N. & Goldstein, S. A. N. KCNKØ: Opening and closing the 2-P-domain potassium leak channel entails 'C-type' gating of the outer pore. *Neuron* 32, 635–648 (2001).

nature COMMUNICATIONS

ARTICLE

Received 19 May 2014 | Accepted 9 Oct 2014 | Published 25 Nov 2014

DOI: 10.1038/ncomms6540

Diacylglycerol mediates regulation of TASK potassium channels by Gq-coupled receptors

Bettina U. Wilke[1], Moritz Lindner[1,†], Lea Greifenberg[1], Alexandra Albus[1], Yannick Kronimus[1], Moritz Bünemann[2], Michael G. Leitner[1] & Dominik Oliver[1]

The two-pore domain potassium (K2P) channels TASK-1 (*KCNK3*) and TASK-3 (*KCNK9*) are important determinants of background K^+ conductance and membrane potential. TASK-1/3 activity is regulated by hormones and transmitters that act through G protein-coupled receptors (GPCR) signalling via G proteins of the $G\alpha_{q/11}$ subclass. How the receptors inhibit channel activity has remained unclear. Here, we show that TASK-1 and -3 channels are gated by diacylglycerol (DAG). Receptor-initiated inhibition of TASK required the activity of phospholipase C, but neither depletion of the PLC substrate $PI(4,5)P_2$ nor release of the downstream messengers IP_3 and Ca^{2+}. Attenuation of cellular DAG transients by DAG kinase or lipase suppressed receptor-dependent inhibition, showing that the increase in cellular DAG—but not in downstream lipid metabolites—mediates channel inhibition. The findings identify DAG as the signal regulating TASK channels downstream of GPCRs and define a novel role for DAG that directly links cellular DAG dynamics to excitability.

[1] Institute of Physiology and Pathophysiology, Department of Neurophysiology, Philipps University, Deutschhausstr. 1-2, 35037 Marburg, Germany. [2] Department of Pharmacology and Clinical Pharmacy, Philipps University, 35032 Marburg, Germany. † Present address: Department of Ophthalmology, University of Bonn, Bonn, Germany. Correspondence and requests for materials should be addressed to D.O. (email: oliverd@staff.uni-marburg.de).

Diacylglycerol (DAG) is one of the best-studied second messengers of eukaryotic cells[1]. It is released by stimulus-induced activation of phospholipase C (PLC), which cleaves the minor plasma membrane phospholipid phosphatidylinositol-4,5-bisphosphate ($PI(4,5)P_2$) to produce DAG and inositol-1,4,5-trisphosphate (IP_3). The PLCβ isozymes are activated by G protein-coupled receptors that signal through the $G_{q/11}$ subclass of Gα proteins (GqPCRs). PLCβ activation occurs by direct interaction with the Gα protein; β/γ subunits and increased intracellular Ca^{2+} can also promote PLCβ activation[2].

As a membrane-resident messenger, DAG operates not only by binding to target proteins, but also by recruiting DAG-binding proteins to the membrane[1,3]. Besides the prototypical DAG effector, protein kinase C (PKC), there is a structural and functional diversity of high-affinity DAG effector proteins[1,4]. However, common to all of these effectors is that the DAG interaction is mediated by cysteine-rich C1 domains, which mediate recruitment to the plasma membrane or activate the protein[5]. Little is known about DAG effectors that do not use C1 domains. Some members of the canonical TRP cation channels (TRPC) can be activated by DAG. The binding site and the molecular mechanism of activation by DAG are unknown[6]. Beyond its function as a messenger in its own right, DAG is also a precursor in the stimulus-driven production of several signalling lipids, including phosphatidic acid (PA), the endocannabinoid 2-arachidonoylglycerol (2-AG), free arachidonic acid and their downstream metabolites[4].

The TWIK-related acid-sensitive K^+ channels, TASK-1 and TASK-3 (KCNK3 and KCNK9), constitute a subgroup of the two-pore domain (K2P) potassium channel family[7]. These channels function as background or 'leak' channels that are open at resting potentials and thus provide a resting K^+ conductance that strongly contributes to setting the membrane potential. In excitable cells TASK channels control action potential threshold and spiking patterns[8–10]. TASK channels show a broad, yet selective expression pattern in many organs, including the central nervous system, peripheral chemoreceptors, vascular smooth muscle and cardiac muscle, and adrenal cortex[7], consistent with the involvement in the regulation of a wide variety of physiological processes.

TASK-1 and -3 channels are extensively modulated by physiological stimuli. A defining property of TASK channels is closure on extracellular acidification near physiological pH[11]. Moreover, they are inhibited by hormones and transmitters that signal through GqPCRs[12–15]. The resulting cellular depolarization is thought to regulate processes such as motor control[10,15,16] and aldosterone secretion[17]. The precise signal-transduction pathway downstream of GqPCRs that operates TASK inhibition has remained unresolved.

Here we show that DAG is both sufficient for TASK channel inhibition and necessary for downregulation by GqPCRs. In contrast, downstream intermediates of DAG had no or only a minor impact on channel activity. The results uncover a new and possibly widespread signalling role for the prototypic lipid messenger DAG. As TASK channels lack the archetypical C1 DAG-binding domain thought to mediate most cellular effects of DAG[1,4], these channels may provide a new paradigm for C1-independent DAG effector proteins.

Results

PLC is required for TASK channel inhibition. Receptor-mediated inhibition of TASK has been proposed to result from either direct interaction with activated $G\alpha_q$[18] or from the action of a messenger downstream of the activity of PLCβ[12,19]. To differentiate between both candidate pathways, we first addressed the requirement for PLCβ in GqPCR-dependent channel inhibition.

We started by testing pharmacological inhibition of PLCβ by the widely used PLC inhibitor U73122 (ref. 20). Application of U73122 almost completely abrogated inhibition of TASK-3 channels in response to activation of the co-expressed Gq-coupled muscarinic M1 receptor (M1R) in Chinese hamster ovary (CHO) cells (Fig. 1a–c). The inactive analogue, U73343, had no effect on receptor-mediated channel inhibition. Because previously reported effects of U73122 on TASK regulation have been controversial[12,18,19,21,22], we additionally controlled for the efficacy of U73122 under our experimental conditions. By using total internal reflection fluorescence microscopy (TIRF-M) measurements with the $PI(4,5)P_2$-binding translocation sensor PLCδ1-PH-GFP as a readout for PLC activity[20,23,24], we confirmed that PLCβ was essentially disabled by preapplication of U73122 (Fig. 1d–f). In this assay the TIRF signal amplitude directly reports the degree of sensor binding to the membrane, and thus the concentration of its ligand $PI(4,5)P_2$. Therefore, fluorescence decrease indicates depletion of $PI(4,5)P_2$ and hence PLC activity. Pre-application of 5 μM U73122, but not U73343, prevented translocation of PLCδ1-PH-GFP from the membrane on activation of M1R. Equivalent results were obtained using a DAG sensor (PKCγ-C1-GFP[20,25]) for detection of PLC activity (not shown).

Previous work addressed the role of PLC by employing a double mutant of $G\alpha_q$ ($G\alpha_q$-AA) thought to disable activation of PLC by active $G\alpha_q$. When expressed in cells lacking both $G\alpha_q$ and $G\alpha_{11}$ ($G\alpha_{q/11}^{-/-}$ embryonic fibroblasts), $G\alpha_q$-AA reconstituted TASK channel inhibition, thus questioning the role of PLC in TASK channel regulation[18]. However, by using PKCγ-C1-GFP as a sensor of PLC activity we found that when expressed in $G\alpha_{q/11}^{-/-}$ cells, $G\alpha_q$-AA efficiently activated PLC on receptor stimulation with little difference to wild-type $G\alpha_q$ (Fig. 1g,h). Further introduction of additional three mutations reported to impair Gq/PLC-coupling ($G\alpha_q$-5A)[26] only slightly affected PLC activation. Accordingly, both $G\alpha_q$ mutants restored receptor-mediated inhibition of TASK-3 in $G\alpha_{q/11}^{-/-}$ fibroblasts (Fig. 1i,j). Recently, Zhang *et al.*[27] developed a chimeric $G\alpha_q$ ($G\alpha_{qiq}$) in which the PLC interaction domain is replaced by the homologous region of $G\alpha_i$. This construct can still be activated by GqPCRs, but coupling to PLC is abrogated. When $G\alpha_{qiq}$ was co-expressed with the M1R receptor and the PKCγ-C1 sensor domain in $G\alpha_{q/11}$-deficient cells, activation of PLC was lacking (Fig. 1g,h), confirming elimination of functional coupling to PLC. As shown in Fig. 1i,j, $G\alpha_{qiq}$ was unable to restore M1R-mediated inhibition of TASK-3 in $G\alpha_{q/11}^{-/-}$ fibroblasts. We therefore conclude that activation of PLC by $G\alpha_q$ is an indispensable step for the receptor-mediated inhibition of TASK channels.

Intracellular Ca^{2+} at or above the physiological resting concentrations is an established requirement for GqPCR-stimulated PLCβ activity[20]. We used this Ca^{2+} dependence as an additional criterion for assessing the involvement of PLC. When intracellular Ca^{2+} was clamped to values below physiological resting levels by inclusion of the Ca^{2+} chelator BAPTA (20 mM) in the intracellular solution, PLC activity, as measured by translocation of the PKCγ-C1 sensor, was indeed abrogated. Receptor-mediated inhibition of TASK-3 channels measured simultaneously from the same cells was also entirely abolished (Fig. 2a). Similarly, 20 mM EGTA largely prevented inhibition of TASK, whereas 5 mM BAPTA only partially occluded channel inhibition (Fig. 2b), which is similar to previous findings showing that buffering with 5 mM BAPTA did not prevent TASK channel regulation[12]. As high buffer concentrations or extremely low intracellular Ca^{2+} levels might

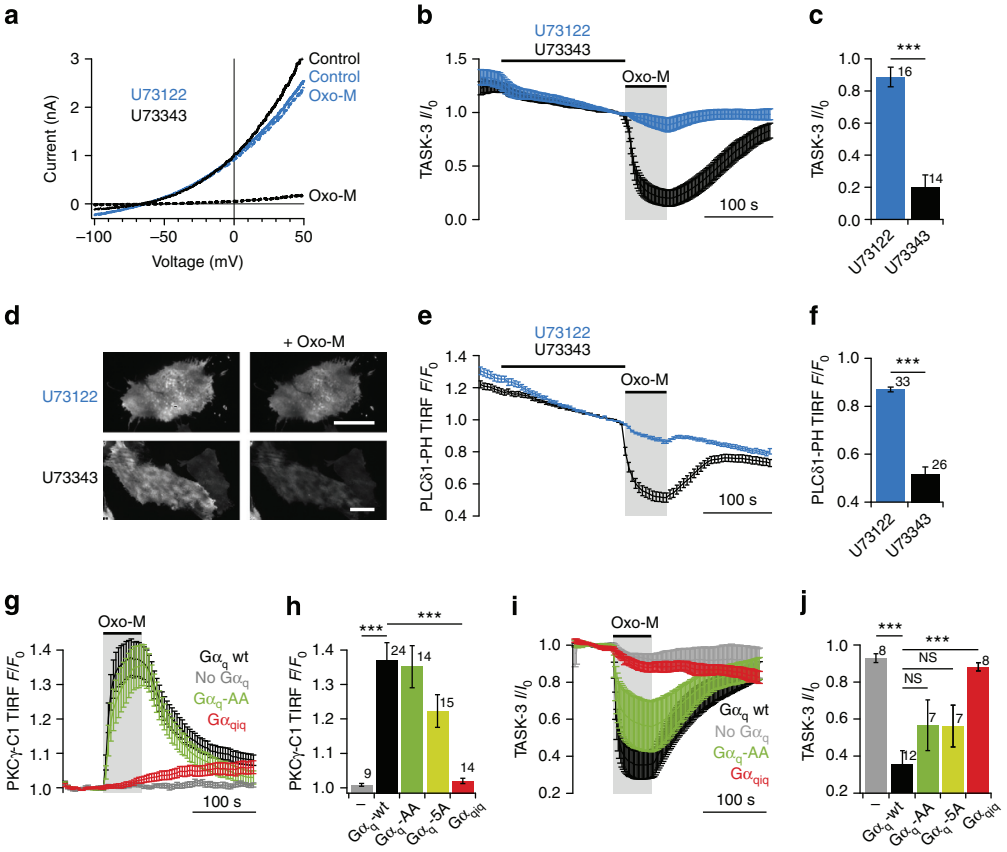

Figure 1 | Phospholipase C (PLC) is necessary for GqPCR-mediated TASK-3 inhibition. (**a**) PLC inhibitor U73122 disabled GqPCR-mediated inhibition of TASK-3. Representative K^+ currents from CHO cells co-transfected with hTASK-3 and M1R before (continuous) and after application of the muscarinic agonist, oxotremorine-M (Oxo-M, 10 μM for all experiments; dashed trace). Recordings were made following application of either 5 μM U73122 (blue) or the inactive analogue U73343 (black). (**b**) Average time course of TASK-3 currents at +50 mV from experiments as in (**a**). Currents were normalized to the amplitude immediately before application of Oxo-M. (**c**) Mean residual currents after application of Oxo-M. (**d**) Inhibition of PLCβ by U73122 was confirmed by the $PI(4,5)P_2$ sensor PLCδ1-PH-GFP. Representative TIRF images of CHO cells co-transfected with PLCδ1-PH-GFP and M1R before (left panels) and during application of 10 μM Oxo-M (right panels). Scale bar, 20 μm. (**e**) Mean time course of single-cell TIRF intensity normalized to fluorescence before application of Oxo-M. (**f**) Mean normalized TIRF intensity at the end of the Oxo-M application. (**g**) M1R-induced activity of PLC was measured in $G\alpha_{q/11}^{-/-}$ fibroblasts co-transfected with DAG sensor PKCγ-C1-GFP, M1R, and either no $G\alpha_q$, wild-type $G\alpha_q$, mutant $G\alpha_q$-AA or a $G\alpha_{qiq}$ chimera deficient in coupling to PLC. PLC activity was probed as the degree of membrane association of PKCγ-C1-GFP with TIRF microscopy. (**h**) Mean normalized increase in membrane association of PKCγ-C1-GFP at the end of the application of Oxo-M in the presence of $G\alpha_q$ or the mutant forms $G\alpha_q$-AA, $G\alpha_q$-5A or $G\alpha_{qiq}$. (**i**,**j**) Differential inhibition of TASK-3 current by receptor activation in $G\alpha_{q/11}^{-/-}$ fibroblasts when co-expressed with either wild type or mutant $G\alpha_q$. Error bars indicate s.e.m. $^{***}P<0.001$; $^{**}P<0.01$; $^{*}P<0.05$. Numbers on bar graphs indicate the number of replicates (individual cells).

also affect other cellular processes, we further tested for the effects of this condition on signalling upstream of PLC activity. To this end we used a FRET assay to monitor receptor-induced interaction between $G\alpha_q$ and PLCβ. As shown in Fig. 2c, the FRET signal between $G\alpha_q$-CFP and YFP-PLCβ3 rapidly increased on activation of co-expressed M1R receptor, directly reporting the interaction. This increase in FRET was not disrupted by high intracellular BAPTA. Thus, upstream signalling including the function of $G\alpha_q$ remained functional, supporting the conclusion that the effect of BAPTA on TASK channel regulation resulted from inhibition of PLC.

Although it had been suggested that depletion of the PLC substrate, $PI(4,5)P_2$, may be the signal triggering channel deactivation[12,28], we recently showed that depletion of $PI(4,5)P_2$ does not alter channel activity of TASK-1 and TASK-3 (ref. 29). Yet, the requirement for PLC implies an indirect role of its substrate $PI(4,5)P_2$, as a sufficient concentration of substrate must be present to allow for the production of any downstream signalling intermediate. We therefore probed the regulation of TASK channels during forced depletion of $PI(4,5)P_2$ and its precursor PI(4)P by pseudojanin, an engineered chimeric phosphoinositide phosphatase that degrades $PI(4,5)P_2$ and PI(4)P[29,30]. Pseudojanin was acutely activated by recruitment to the membrane via rapamycin-dependent heterodimerization (Fig. 2d)[29,31]. Pseudojanin-mediated depletion of $PI(4,5)P_2$ and PI(4)P precluded PLC activity on subsequent activation of M1R as indicated by lack of DAG production (Fig. 2e) and abolished channel inhibition (Fig. 2f). As it was previously shown that transcriptional induction of a $PI(4,5)P_2$ 5-phosphatase did not affect regulation of TASK currents by G_q-coupled receptors[18], we also tested for an effect of selective depletion of $PI(4,5)P_2$. To this end we used a pseudojanin construct in which the PI(4)P 4-phosphatase SAC1 was inactivated by mutation (PJ-5Ptase). As shown in Fig. 2f, recruitment of PJ-5Ptase did not affect TASK regulation. However, monitoring the production of DAG under this condition revealed that the receptor-induced DAG transient was also unchanged (Fig. 2e). Thus, despite depletion of $PI(4,5)P_2$, PLC activity is not reduced to a measurable degree. Selective activation of a 5-phosphatase may not be sufficient to lower $PI(4,5)P_2$ concentration enough to eliminate $PI(4,5)P_2$

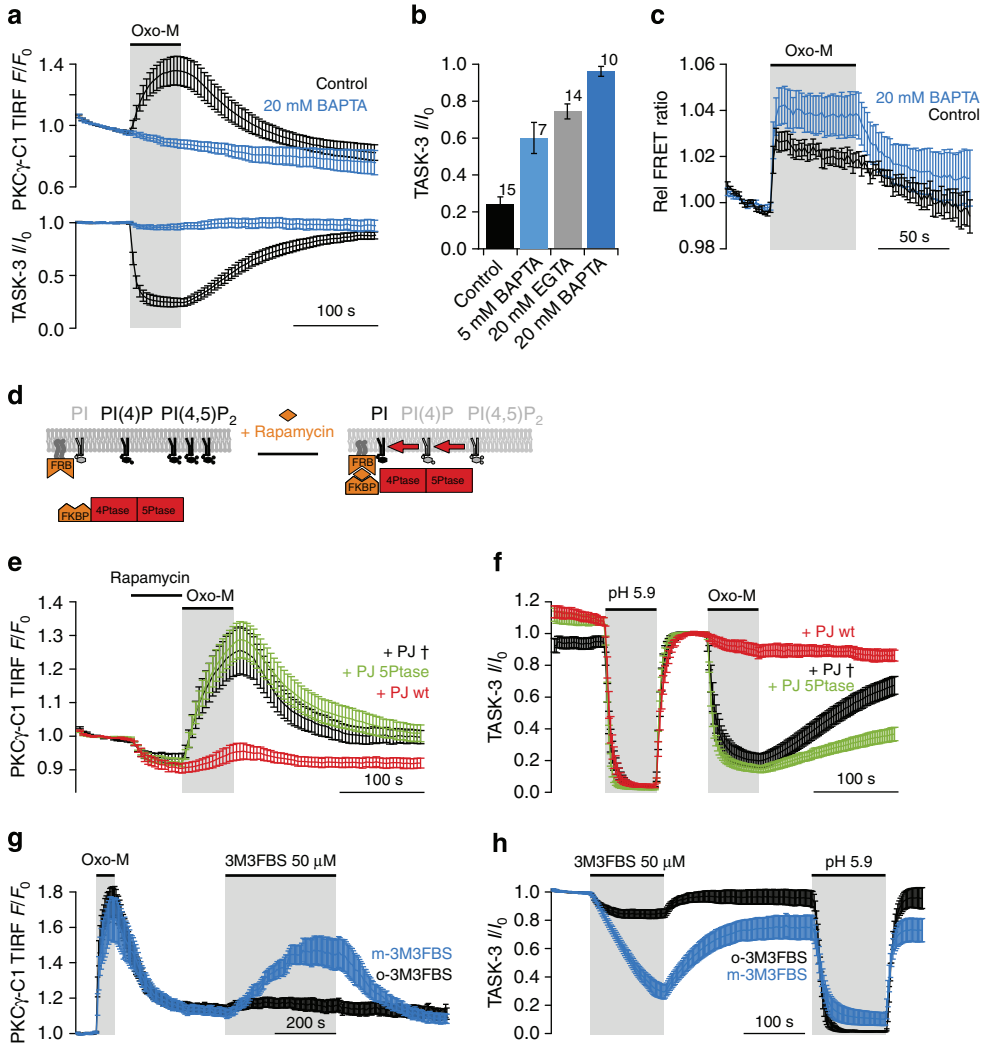

Figure 2 | Involvement of PLC in GqPCR-mediated TASK-3 inhibition. (**a**) Strong buffering of intracellular Ca^{2+} suppressed TASK-3 inhibition by M1R. CHO cells co-expressing TASK-3, DAG sensor PKCγ-C1-GFP and M1R were whole-cell patch-clamped with intracellular solutions buffered to either 0.1 µM free Ca^{2+} (control) or without Ca^{2+} but 20 mM of the Ca^{2+} chelator BAPTA. PKCγ-C1-GFP translocation was monitored simultaneously by TIRF microscopy. (**b**) Mean residual currents after application of 10 µM Oxo-M with either 0.1 µM intracellular Ca^{2+} (control) or the Ca^{2+} chelators indicated. (**c**) Dynamic FRET measurements between $G\alpha_q$-CFP and YFP-PLCβ3 were done with whole-cell patch-clamped cells after 4 min of equilibration with solutions containing either 0.1 µM free Ca^{2+} (control, $n=9$) or 20 mM BAPTA ($n=9$). Rapid increase in FRET following activation of co-expressed M1R indicates comparable association of $G\alpha_q$ and PLCβ3 in both conditions. (**d**) Principle of induced depletion of PLC substrate. Application of rapamycin triggers heterodimerization of FRB/FKBP, leading to irreversible recruitment of pseudojanin (PJ) to the plasma membrane. PJ comprises a 4-phosphatase and 5-phosphatase domain, degrading both $PI(4,5)P_2$ and PI(4)P. (**e**) PLC-mediated DAG production was blocked by recruitment of PJ ($n=16$), but not catalytically inactivated PJ (PJ†; $n=24$) or PJ with exclusive 5-phosphatase activity (PJ 5Ptase; $n=36$). Cells were co-transfected with PKCγ-C1-GFP, M1R, Lyn11-FRB and PJ variants fused to mcherry-FKBP. Cells were selected for membrane recruitment of mcherry. (**f**) Recruitment of PJ, ($n=14$), but not PJ-5Ptase ($n=9$) or catalytically inactive PJ† ($n=12$), suppressed current inhibition by M1R without affecting channel gating by extracellular acidification. Cells were co-transfected with TASK-3, M1R, Lyn11-FRB and PJ variants. Rapamycin (5 µM) was applied before the experiments shown. Cells were selected for membrane translocation of mcherry, or for PJ wt for translocation of co-expressed PLCδ1-PH-GFP, indicating depletion of $PI(4,5)P_2$. (**g**) m-3M3FBS induced translocation of the DAG sensor PKCγ-C1-GFP, indicating reversible activation of PLC ($n=20$ cells from three experiments). The inactive analogue o-3M3FBS was largely ineffective ($n=15$ cells from three experiments). (**h**) Application of m-3M3FBS ($n=9$) but not o-3M3FBS ($n=7$) reversibly inhibited TASK-3 current. Error bars indicate s.e.m.

turnover by PLC, perhaps because some $PI(4,5)P_2$ is continuously resynthesized from the augmented PI(4)P pool. Alternatively, PI(4)P may itself also be a relevant substrate of PLCβ[20]. In conclusion, the requirement of $PI(4,5)P_2$ and PI(4)P for TASK channel regulation by GqPCRs but not for basal channel activity corroborates the role of PLC activity in TASK regulation.

We next asked whether PLC activity is also sufficient for inhibiting TASK channels. To this end, we used the benzenesulfonamide m-3M3FBS that activates PLC independent of GqPCRs[20,32]. According to plasma membrane translocation of the DAG sensor PKCγ-C1 m-3M3FBS, but not its inactive analogue o-3M3FBS, activated PLC when applied to CHO cells (Fig. 2g). The kinetics and amplitude of sensor translocation indicated that activation of PLC by m-3M3FBS occurred more slowly and was somewhat weaker compared with PLC activity triggered by M1R. As shown in Fig. 2h, application of m-3M3FBS robustly inhibited TASK-3 currents, whereas the inactive analogue had little effect. Current inhibition developed slowly,

was slowly reversible and was less complete compared with receptor activation, mirroring the characteristics of PLC activation as monitored with the fluorescent sensor of PLC activity.

Taken together, these data demonstrate that activation of PLCβ is an essential requirement for inhibition of TASK-3 channels by a G_q-coupled receptor and that activation of PLC is sufficient to induce channel inhibition. Hence, the signal that mediates channel closure must be downstream of PLCβ.

Diacylglycerol inhibits TASK channels. To identify the relevant biochemical signal, we next directly applied candidate downstream messengers to TASK channels. Application of the membrane permeable short-chain DAG analogue 1,2-Dioctanoyl-*sn*-glycerol (DiC8)[25] to CHO cells expressing TASK-3 or TASK-1 resulted in dose-dependent and reversible current inhibition (Fig. 3a,b). At the same concentration range, DiC8 induced robust but sub-maximal translocation of the DAG sensor domain PKCγ-C1-GFP to the plasma membrane (Fig. 3c), suggesting that the concentrations reached by exogenous application may be comparable to cellular concentrations of endogenous DAG produced on stimulation of GqPCRs.

As shown in Fig. 3d,e, application of DiC8 to the cytoplasmic face of giant patches excised from *Xenopus* oocytes similarly inhibited TASK-3 activity. The effectiveness in this cell-free condition points to a direct action of DAG on the channel and argues against an involvement of DAG-dependent protein kinase (PKC) or of DAG metabolites. The inside-out configuration of the giant patch also allowed for the direct delivery of 'native' long-chain DAG to the inner leaflet of the membrane (Fig. 3d-f). Endogenous DAG produced by PLCβ is predominantly 1-stearoyl-2-arachidonoylglycerol (SAG)[33]. Application of SAG (20 μM) to giant patches produced a potent inhibition of TASK-3, with an efficacy slightly greater than the short-chain analogue DiC8 at the same concentration (Fig. 3d,e). Channel inhibition was dose-dependent with a half-inhibiting concentration of about 10 μM (Fig. 3f). Inhibition was poorly reversible, presumably because partitioning of SAG into the plasma membrane is not readily reversible.

We further tested the lipid metabolites 2-arachidonoyl-glycerol (2-AG) derived from DAG by diacylglycerol lipases (DGLs), and

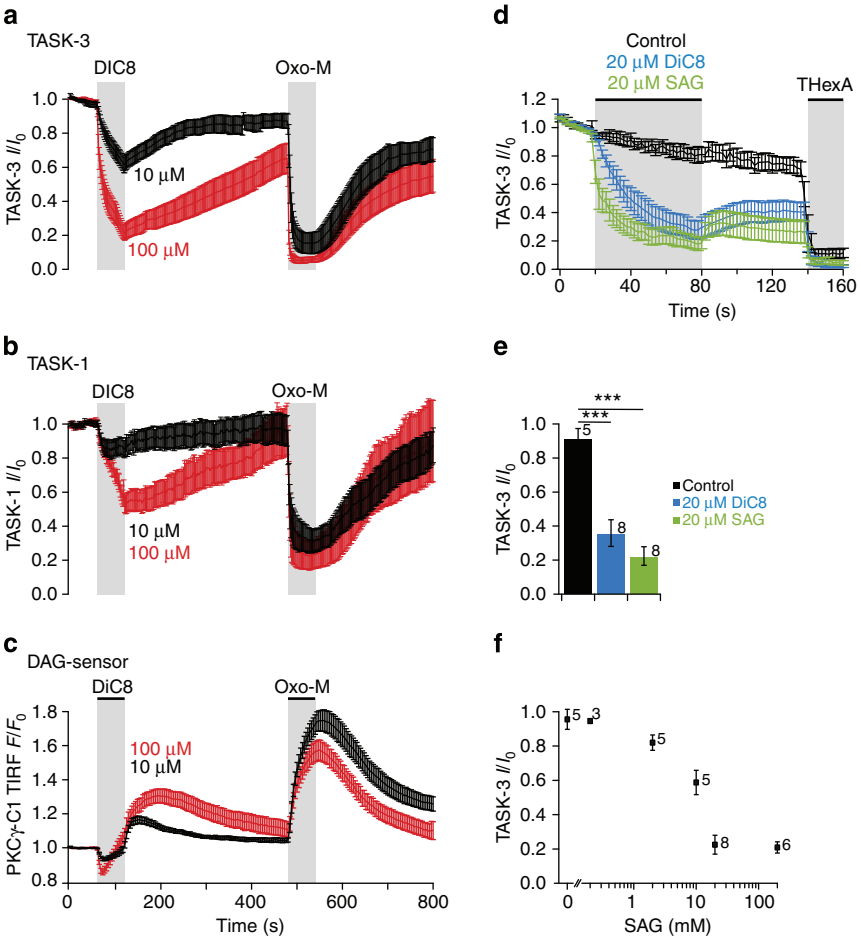

Figure 3 | DAG directly inhibits TASK-1 and -3 channels. (**a**) Application of short-chain DAG analogue (1,2-dioctanoyl-*sn*-glycerol; DiC8) onto CHO cells reversibly inhibited TASK-3; $n=7$ both for application of 10 μM (black) and 100 μM DiC8 (red). (**b**) Application of 10 μM ($n=8$) or 100 μM ($n=6$) DiC8 to CHO cells expressing TASK-1. (**c**) Membrane association of DAG sensor PKCγ-C1-GFP induced by application of DiC8 to CHO cells (10 or 100 μM; $n\geq 29$ cells from ≥ 6 experiments, each). Activation of the co-expressed M1R by 10 μM Oxo-M served as a control for strong DAG production. (**d**) Application of DiC8 and 1-Stearyl-2-arachidonoyl-*sn*-glycerol (SAG) inhibited TASK-3 channels when applied to the intracellular face of giant inside-out patches excised from *Xenopus* oocytes. Tetrahexylammonium (THexA; 10 μM) completely blocking the channel was applied to gauge overall TASK-3 currents. Shown are mean currents measured at +50 mV at the end of each repetitive voltage ramp, normalized to current size before application ($t=30$ s). (**e**) Residual TASK-3 currents at the end of the DAG application from experiments in (**d**). *** indicates $P<0.001$. (**f**) Dose-dependent inhibition of TASK-3 currents by SAG, measured in giant patches as in (**d**,**e**). Data are presented as mean ± s.e.m.

phosphatidic acid (PA) generated by phosphorylation of DAG through diacylglycerol kinases (DGKs)[4]. Consistent with a previous report[34], the endocannabinoid 2-AG also inhibited TASK-3, albeit with a lower efficacy compared with SAG (Fig. 4a,b). PA or arachidonic acid (AA), which can be released from 2-AG, had little effect on channel activity.

Application of either IP_3 or Ca^{2+} to TASK-3 had no effect on channel activity (Fig. 4c,d), indicating that the IP_3/Ca^{2+} branch of the PLC-dependent signal-transduction cascade is not involved in TASK regulation by GqPCRs.

DAG dynamics mediate receptor-induced TASK inhibition. These results indicated DAG as a likely messenger mediating TASK channel modulation. We therefore asked whether DAG indeed mediates channel inhibition in response to GqPCR activity. We aimed at altering cellular DAG dynamics and reasoned that accelerating the turnover of DAG should reduce the DAG concentrations reached on receptor stimulation. Cellular DAG accumulating on activation of PLCβ is cleared by DGKs or by DGLs[4]. Among the 12 isoforms of DGK we found DGKβ to be constitutively localized at the plasma membrane when overexpressed in CHO cells (Fig. 5a inset), suggesting that it may effectively turn over DAG after receptor activation. Indeed, expression of DGKβ strongly blunted the receptor-induced DAG transient in CHO cells (Fig. 5a,c). When co-expressed with TASK-3 channels, DGK similarly suppressed channel inhibition by activation of M1R (Fig. 5d,f). Overexpression of DAG lipase alpha (DGLα[35]) also strongly attenuated the receptor-induced accumulation of DAG (Fig. 5b,c). As shown in Fig. 5e,f, DGLα also suppressed receptor-mediated channel inhibition and accelerated current recovery when co-expressed with TASK-3 channels.

These findings are consistent with DAG acting as the endogenous messenger that inhibits TASK channels. At the same time, the results rule out a major role of downstream lipid messengers in inhibiting TASK channels, including PA and 2-AG and its metabolites, as their concentrations should be increased rather than decreased by DGK and DGL, respectively. We note that the impairment of current inhibition by DGLα appears less pronounced than the decrease in the DAG transient reported by the PKCγ-C1-GFP sensor. However, the remaining channel inhibition may be readily explained by weak inhibition of TASK by the DGL product 2-AG, as observed in isolated patches (Fig. 4a).

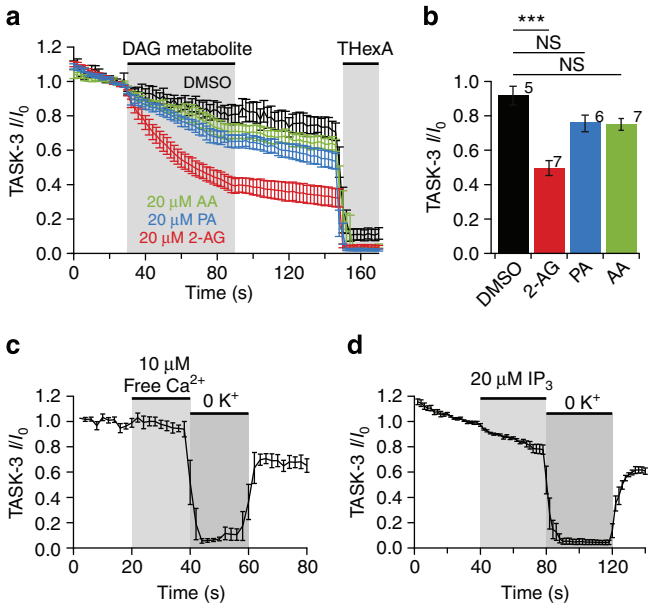

Figure 4 | DAG metabolites, IP_3 and intracellular Ca^{2+} have little effect on TASK-3 channel activity. (**a**) Effects of DAG metabolites on TASK-3 currents in giant inside-out patches from *Xenopus* oocytes. Control data with application of vehicle (DMSO) is replotted from Fig. 3d for comparison. (**b**) Mean residual TASK-3 currents measured at the end of the application of the various lipids from experiments in (**a**). (**c**) Application of 10 µM free Ca^{2+} to the intracellular face of giant patches was without effect on TASK-3 currents ($n=6$). Currents measured as in (**a**). Subsequent removal of intracellular K^+ completely eliminated K^+ outward currents, verifying that currents were mediated by TASK-3. (**d**) Application of 20 µM IP_3 ($n=7$) to inside-out patches did not inhibit TASK-3 currents. Giants patch recordings were done as in (**a**) and (**c**). Data are presented as mean ± s.e.m.

A proximal C-terminal motif essential for inhibition by DAG. A six-amino-acid motif (VLRFLT) located at the proximal C terminus of TASK-3 channels is essential for the channels' sensitivity to GqPCR modulation[14]. If DAG mediates the receptor's effect, the same motif must also determine the sensitivity to exogenous DAG. We therefore next examined TASK channels with mutation or deletion of the short motif (Fig. 6a). Figure 6b shows that truncation of the C terminus of TASK-3 preserving the VLRFLT motif (Δ249) yielded functional channels still sensitive to regulation by GqPCRs, consistent with previous findings[14]. However, additional removal of the VLRFLT motif (Δ244) rendered the channel insensitive to activation of the co-expressed receptor. These channels were still gated by extracellular pH, indicating that the fundamental function of the truncated channels was not compromised. Strikingly, the sensitivity of these truncated channels to DAG mirrored their inhibition by the GqPCR. Thus, inhibition by DiC8 (20 µM) was unchanged in Δ249, but was abrogated by truncation of the VLRFLT motif (Fig. 6c).

We further analysed the relevance of this motif by replacing individual amino acids by alanine. As shown in Fig. 6d, these mutations impaired GqPCR-dependent regulation to different degrees, with the most pronounced effects observed in the L244A and R245A mutants. When challenged with DiC8, the resulting channel inhibition of L244A and R245A was also largely reduced (Fig. 6e). Overall, inhibition by DiC8 of the various mutant channels correlated well with their sensitivity to receptor activity (Fig. 6f).

In conclusion, inhibition of TASK channels by DAG relies on the same molecular determinants that govern inhibition by Gq signalling, lending further support to the conclusion that receptor/Gq-induced TASK channel inhibition is mediated by increased DAG levels.

DAG inhibits TASK currents in cerebellar granule neurons. Regulation of TASK channels by Gq-coupled receptors strongly impacts on membrane potential and excitability in many cell types. In cerebellar granule neurons (CGNs), a large 'standing outward' current (IK_{SO}) dominated by TASK-1 and TASK-3 channels[36–38] controls resting potential and action potential firing[8,36,38]. Gq-coupled neurotransmitter receptors (including muscarinic acetylcholine receptors and metabotropic glutamate receptors) dynamically regulate CGN excitability by inhibition of TASK channels[12,39].

We examined the activity of short-chain DAG, DiC8, on IK_{SO} in dissociated cultured CGNs. Application of DiC8 (100 µM) reduced the outward current by about 50%, similar to current suppression by extracellular acidification or activation of endogenous muscarinic acetylcholine receptors (Fig. 7a,b). As CGNs express other K2P channels in addition to TASK[40], we combined extracellular acidification with application of DAG

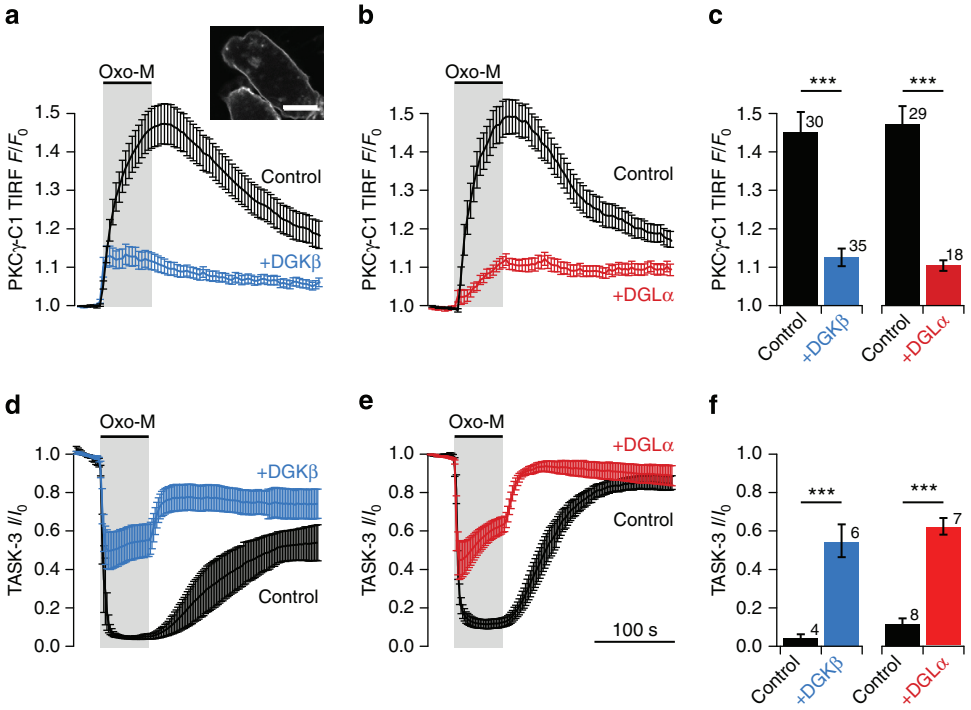

Figure 5 | Suppression of cellular DAG-transients attenuates receptor-mediated TASK-3 inhibition. (**a**) DAG concentration dynamics in CHO cells induced by M1R (10 μM Oxo-M) were measured by TIRF microscopy of PKCγ-C1-GFP either in the absence (control) or with co-expression of DAG-kinase β (DGKβ). Confocal image (inset) shows membrane localization of GFP-tagged DGKβ (Scale bar, 10 μm). (**b**) Receptor-induced DAG dynamics measured as in (**a**) either without (control) or with co-expression of DAG lipase α (DGLα). (**c**) Mean TIRF signal increase (± s.e.m.) at the end of 60 s Oxo-M application from experiments shown in (**a**) and (**b**). Numbers indicate individual recordings. (**d**) TASK-3 current inhibition by activation of M1R with or without co-expression of DGKβ. (**e**) TASK-3 current inhibition by activation of M1R with or without co-expression of DGLα. (**f**) Mean residual TASK-3 currents at the end of Oxo-M application from the experiments shown in (**d**,**e**). Current inhibition was strongly reduced by either DGKβ or DGLα, matching the suppressed DAG transients (**a**–**c**).

to test whether the DAG-sensitive currents correspond to neuronal TASK channels. As shown in Fig. 7c, only a minor fraction of residual IK_{SO} remained sensitive to DAG when TASK currents were blocked by pH 5.9 and acid-sensitive TASK currents remained closed when switching back to pH 7.4 after exposure to DAG. These observations support the conclusion that most of the DAG-sensitive currents in CGNs was indeed mediated by TASK. Taken together, these findings suggest that the current component carried by TASK channels is sensitive to DAG, consistent with the idea that the inhibition of native TASK channels by neuronal GqPCRs is indeed mediated by DAG.

Application of DAG also depolarized the membrane potential of CGNs by about 10 mV (Fig. 7d,e), similar to activation of endogenous ACh receptors, indicating that DAG-mediated regulation of TASK channels underlies modulation of neuronal electrical excitability.

Discussion

Here, we show that GqPCRs inhibit TASK channels through the production of DAG. Thus, several independent assays indicated that PLC activity is essential for channel inhibition. Among the downstream messengers of PLC, only DAG induced channel inhibition. Moreover, accelerating the turnover of DAG by overexpression of either DGK or DGL suppressed channel inhibition, demonstrating that liberation of DAG is indeed necessary for channel regulation.

TASK channels are inhibited by DAG and not through messengers downstream of DAG, as DAG application rapidly inhibited channels in a cell-free system (excised patch), where recruitment of cytoplasmic DAG effectors, activation of kinase signalling, or conversion of DAG to downstream messengers is unlikely. In principle DAG could act on TASK channels via activation of protein kinase C (PKC), as pharmacological activation PKC can modulate TASK channels[41]. However, several careful studies consistently found that PKC does not mediate GqPCR-induced inhibition. Thus, neither removal of all potential PKC phosphorylation sites[14,41] nor pharmacological blockade of PKC[12,19,22,41] affected receptor-dependent channel regulation. This is in line with our current results showing that DAG is effective in isolated patches and inhibits truncated channels lacking potential PKC phosphorylation sites.

The model that follows is direct binding of DAG to the channel. This could be binding of DAG directly either to the pore-forming α-subunits or to an accessory protein that is present in the plasma membrane and interacts with the α-subunit. We consider direct binding to the channel as the more simple and straightforward model, since (i) to our knowledge, appropriate interaction partners of TASK-1/3 are not known, (ii) the C-terminally truncated TASK channel should be deprived of much of its potential cytoplasmic protein–protein interaction interfaces and (iii) a relevant accessory protein would have to be ubiquitously and abundantly expressed in plasma membranes as DAG was effective in a wide variety of cells ranging from *Xenopus* oocytes to neurons; in fact, GPCR-mediated TASK channel inhibition is reported to work in essentially any cell type examined.

As enzymatic conversion of DAG into PA or 2-AG reduced channel inhibition, these downstream intermediates cannot mediate channel inhibition. It is worth noting, however, that in the excised patch, 2-AG also inhibited TASK channels and that increased conversion of DAG to 2-AG did not fully block

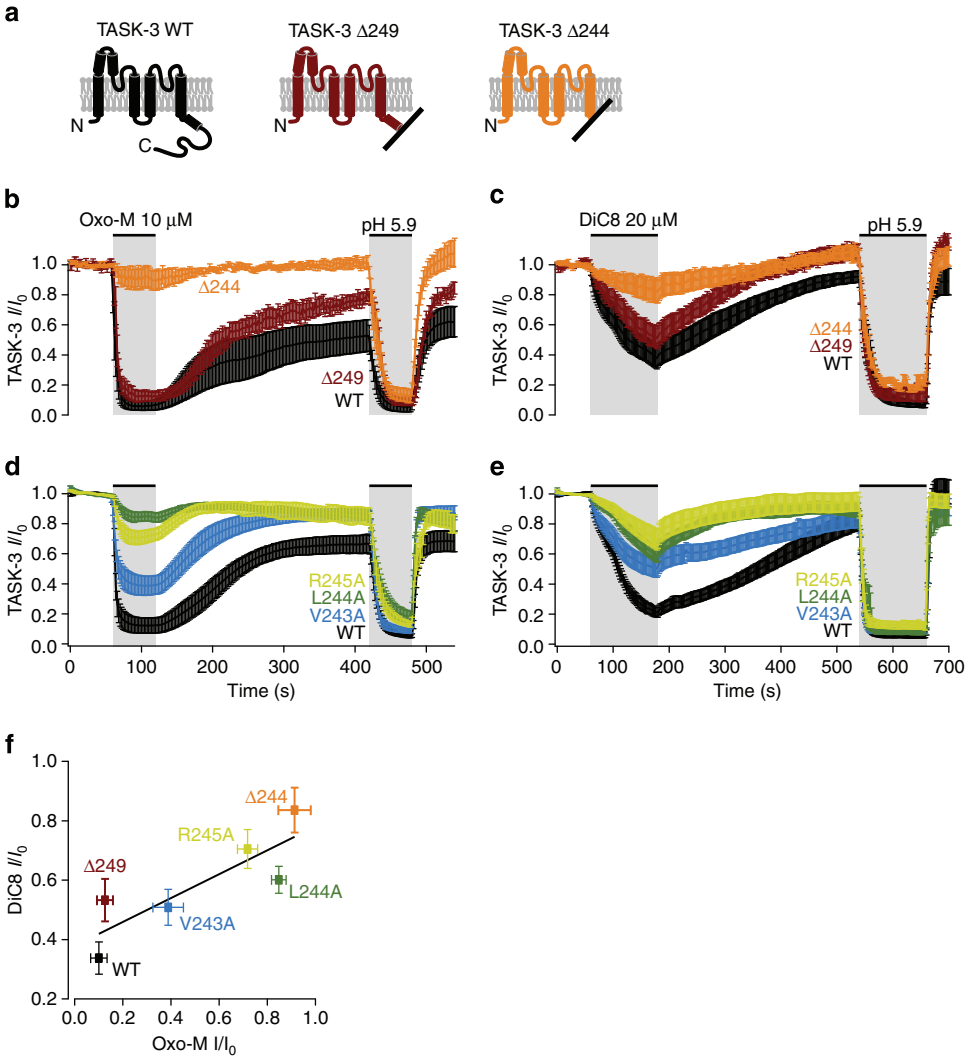

Figure 6 | The C-terminal VLRFLT motif is critical for DAG-mediated channel inhibition. (**a**) Schematic representation of C-terminal channel truncations: TASK-3 was truncated either after position 248, retaining the VLRFLT motif, (TASK-3 Δ249) or after position 243, removing the entire C terminus (TASK-3 Δ244). (**b**) Removal of the VLRFLT motif rendered TASK-3 currents insensitive to co-expressed G_q-coupled M1R, whereas truncation after this motif had no effect on channel regulation ($n=6$, 7 and 5 cells, for wt, Δ249, and Δ244 channels, respectively). Inhibition by extracellular acidification demonstrated that currents were carried by TASK-3 and confirmed functional integrity of truncated channels. (**c**) Whole-cell recordings of the effect of DiC8 on TASK-3 and truncated channels ($n=9$, 9 and 7 cells, for wt, Δ249 and Δ244 channels, respectively) expressed in CHO cells. (**d**) Point mutations in the VLRFLT motif reduced the channel sensitivity towards M1R-mediated inhibition ($n=11$, 10, 10, 11 cells for wt, V243A, L244A and R245A, respectively). (**e**) Channel mutants with attenuated receptor-induced inhibition also showed reduced sensitivity towards application of 20 μM DiC8 ($n=5$, 7, 7 and 5 cells for wt, V243A, L244A and R245A, respectively). (**f**) Correlation of channel inhibition by M1R receptor versus application of DiC8, derived from the experiments presented in (**b**–**e**). Shown are normalized current amplitudes at the end of the application of Oxo-M or DiC8 (mean ± s.e.m.).

receptor-induced channel inhibition, although the DAG transient was strongly attenuated. Thus, production of 2-AG may also make a minor contribution to TASK channel regulation by GqPCRs.

It was proposed previously that TASK inhibition is mediated by direct interaction with activated $G\alpha_q$ rather than by downstream signals[18]. In particular a direct biochemical interaction between $G\alpha_q$ and the TASK channel supports such a mechanism. However, as the various independent approaches blocking PLC function all abolished receptor-dependent inhibition it seems highly unlikely that $G\alpha_q$ alone could be sufficient to inhibit TASK channels. On the contrary, DAG by itself is sufficient to downregulate the channels. Yet it remains possible that $G\alpha_q$ could contribute to channel inhibition by increasing DAG affinity or efficacy through direct TASK-$G\alpha_q$ interaction, although such a model is speculative at present.

Although the control of TASK-1/3 by DAG has not been recognized before, it is well established that other lipid compounds inhibit these channels. The endocannabinoid anandamide and its synthetic analogue methanandamide potently inhibit TASK channels by direct interaction with the channel[34,42]. Our current finding of partial inhibition by 2-AG suggests another endocannabinoid as a regulator of these background channels. Notably, all these compounds are chemically similar to DAG in consisting of arachidonic acid bound to a small moderately polar headgroup containing a hydroxyl group. It thus seems likely that all of these compounds share a common mechanism of TASK inhibition. It is further interesting to note that sanshool, the pungent compound of Szechuan pepper, acts by inhibiting TASK channels[43]. Sanshool is chemically similar to the aforementioned compounds in being an amide of a

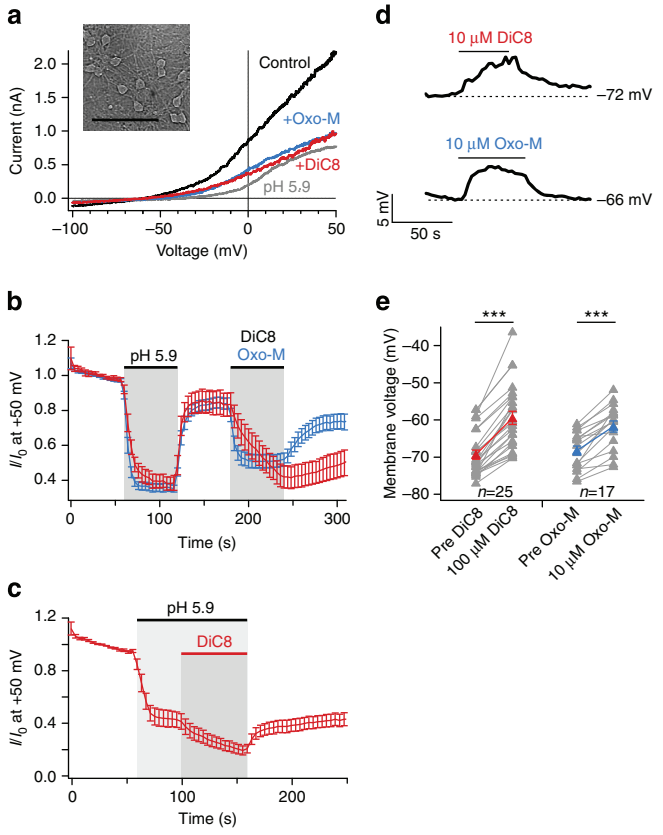

Figure 7 | Inhibition of native IK_{SO} in cerebellar granule cells by DAG. (**a**) Representative whole-cell currents from a dissociated cerebellar granule cell (inset; scale bar, 50 μm). Currents were recorded in response to voltage ramps from a holding potential of +50 mV. Application of 10 μM Oxo-M to activate endogenous muscarinic receptors or 100 μM DiC8 inhibited outward potassium currents to a similar extent as extracellular acidification to pH 5.9. (**b**) Mean time course of standing outward currents during application of 10 μM Oxo-M ($n=18$) or 100 μM DiC8 ($n=7$), and extracellular acidification. Currents were measured at +50 mV and normalized to current amplitude before initial acidification. (Error bars indicate s.e.m.). (**c**) Mean time course of IK_{SO} in response to combined application of low extracellular pH and DiC8 (100 μM). (**d**) Representative recordings of membrane potential during application of DiC8 (upper trace) or Oxo-M (lower trace). (**e**) Change of membrane potential induced by application of DiC8 ($\Delta V_m = 9.9 \pm 0.9$ mV) or muscarinic receptor stimulation ($\Delta V_m = 6.5 \pm 0.8$ mV) from experiments performed as in (**d**). *** indicates $P<0.001$ tested with a paired Student's *t*-test.

polyunsaturated fatty acid and a moderately polar alcohol. It is tempting to speculate that sanshool elicits sensory effects by hijacking a binding site at TASK channels built for regulation via endogenous lipid messengers.

All well-characterized DAG effectors are earmarked by containing at least one prototypical C1 DAG-binding domain. Among the C1-containing proteins, the PKCs are often considered as the canonical and most important DAG effectors. Additional protein families containing C1 domains are the chimaerins, DGKs, protein kinase D and Munc13s[1,4]. In contrast, TASK channels do not contain a C1 domain. DAG also contributes to the activation of certain canonical TRP (TRPC) channels[6,44], which also lack a C1 domain. To our knowledge, the binding site for DAG has not been identified.

Our data show that a six-amino-acid motif (VLRFLT) at the most proximal intracellular C terminus of TASK-3 is crucial for DAG inhibition. Although its location close to the membrane's inner leaflet may suggest a role in DAG binding, the membrane-proximal C terminus is implicated in gating of other K2P channels by a variety of stimuli. In TREK channels it mediates channel gating by phospholipids, membrane tension, intracellular pH and the antidepressant fluoxetine[45–47]. In TASK channels, the VLRFLT motif is also essential for channel activation by volatile anaesthetics[14]. Thus, it seems that the VLRFLT motif is most likely a gating element coupling DAG binding to channel closure; however, it is also possible that it contributes to binding of DAG. Yet, it remains to be shown if DAG indeed binds directly to the channel's pore-forming subunit. If so, the fact that even the truncated minimalistic channel remains sensitive to DAG should facilitate identification of the DAG binding sites in TASK channels; the only intracellular structures to be considered as potential interaction sites of the headgroup of membrane-embedded DAG remaining in truncated TASK channel are the VLRFLT motif, a short N terminus of seven amino acids, and an intracellular loop of some 30 amino acids connecting M2 and M3. Thus, TASK channels may be amenable to the study of structural details of DAG binding and may serve as a novel paradigm for DAG effector molecules not operated via C1 domains.

How might DAG alter gating to close the channels? Ashmole *et al.*[48] hypothesize that the underlying gating mechanism may be related to the gating by voltage, where depolarization increases open probability. Future single channel studies may provide more insights into the mechanistic details.

Our results establish the control of K2P channels as a novel signalling role for DAG. Given the widespread expression of TASK channels and their established functions[7], for example, in neurons[9,15,38] and adrenocortical cells[17], this new signalling pathway is most likely important in many physiological processes. The tight regulation of plasma membrane DAG concentrations may be critical for maintaining appropriate TASK channel activity. Specifically, DAG concentration dynamics triggered by PLC activation depend on the rate of DAG clearance. Among the 10 mammalian DGK isoforms, several have been associated with the control and termination of PLC/DAG signalling in the plasma membrane[4,49]. Interestingly, mutation of DGKδ, one of DGK isoforms prominently expressed in the brain, is associated with epilepsy in humans and mice[50]. In principle, such a phenotype might result from excessive suppression of a potassium conductance by increased DAG levels. Knock-out of other neuronal DGKs also leads to neuronal and behavioural alterations that are linked to changed DAG signalling[51,52]. It should be interesting to examine whether dysregulation of TASK channel activity plays a role in these pathologies. DAG is also turned over by DGLs to generate the endocannabinoid 2-AG. Although their signalling function has been considered mostly in terms of production of the signalling lipids 2-AG and AA[35], a role in regulating TASK channels by curtailing DAG signals should be considered, given that experimental overexpression of DGLα strongly affected DAG transients (Fig. 5).

In summary, our findings indicate that DAG dynamics and homeostasis directly control a multitude of cellular processes dependent on membrane potential, such as neuronal excitability, muscle contraction and hormone secretion through the inhibition of TASK-1 and -3 channels.

Methods

Cell culture. CHO dhFr$^-$ cells were grown at 37 °C with 5% CO_2 in minimum essential medium (MEM)-α with nucleosides supplemented with 10% fetal calf serum (Biochrom AG, Berlin, Germany), 100 U ml^{-1} penicillin and 100 μg ml^{-1} streptomycin. $G\alpha_{q/11}{}^{-/-}$ fibroblasts (kindly provided by Douglas A. Bayliss) were cultured at 37 °C with 5% CO_2 in Dulbecco's modified eagle medium (DMEM) with high glucose and GlutaMax supplemented with 10% fetal calf serum (Biochrom AG), 100 U ml^{-1} penicillin and 100 μg ml^{-1} streptomycin. Both cell lines were seeded onto glass coverslips or glass-bottom dishes (WillCo Wells B.V.,

Amsterdam, The Netherlands) for electrophysiology and imaging experiments, respectively. One to two days after seeding cells were transfected using JetPEI (Polyplus Transfection, Illkirch, France) according to the manufacturer's protocol. Experiments were performed 24–72 h post transfection.

CGNs were prepared from P6-P9 Wistar rats. Animals were anaesthetized and decapitated to obtain cerebella, which were washed in ice-cold PBS, cut in 3–4 pieces and incubated at 37 °C for 15 min in 0.05% trypsin-EDTA/HBSS. After washing with DMEM, cerebelli were incubated with 10% DNase I (Sigma-Aldrich, Taufkirchen, Germany)/DMEM at 37 °C for 4 min. Cells were then triturated using fire-polished glass Pasteur pipettes with decreasing openings, passed through a 70-µm cell strainer and washed in a centrifugation step of 10 min at 210 *g* at 4 °C. CGNs were resuspended in DMEM with high glucose and GlutaMax supplemented with 10% horse serum (Biochrom AG), 100 U ml^{-1} penicillin and 100 µg ml^{-1} streptomycin and 25 mM KCl and plated on poly-D-lysine coated (MW 70,000-150,000; Sigma-Aldrich) glass coverslips with a density of 400,000 cells per cm^2. After 1 h of cell sedimentation, 1 µM cytosine β-D-arabinofuranoside (Sigma-Aldrich) was added to the medium to prevent glial growth. Neurons were used for whole-cell recordings after 7–12 days in culture.

Media and buffers used for cell culture were obtained from Gibco (Life Technologies, Carlsbad, CA, USA) unless noted otherwise.

Molecular biology. The following expression plasmids were used for transient transfection of CHO cells or $G\alpha_{q/11}{}^{-/-}$ fibroblasts: rat PKCγ-C1 (AA 26-89 in pEGFP-N1 NM_012628.1; obtained from Tobias Meyer); human PLCδ1-PH (AA 1-170 in pEGFP-N1; NM_006225.3, obtained from Tamas Balla); mouse $G\alpha_q$ (in pcDNA3, CFP inserted between AA 124/125 (ref. 53); NM_008139.5); mutant $G\alpha_q$ constructs $G\alpha_q$-AA and $G\alpha_q$-5A contain the point mutations R256A/T257A or DNE243-245AAA/R256A/T257A, respectively; human $G\alpha_{qiq}$ (chimera of Gαq AA 1-245 + AA 333-359; NM_002072.4 and Gαi AA 242-328; NM_002070.3 in pcDNA3.1; kind gift from Xuming Zhang); human TASK-1 (in pcDNA3.1; NM_002246.2), human TASK-3 (in pcDNA3.1; NM_001282534.1; obtained from Jürgen Daut); human M1 receptor (in pSGHV0; NM_000738.2), rat DGKβ (in pEGFP-C3, GFP was removed for TIRF experiments; NM_019304.1, kindly provided by Fumio Sakane); human DGLα-GFP (in pcDNA3.1/V5-His TOPO; NM_006133.2, gift from Patrick Doherty); mcherry-FKBP-Pseudojanin (in pEGFP-C1; AA 30-108 of FKBP NM_054014.3, AA 2-517 of SAC1 NM_001179777.1, AA 214-644 of InPP5E NM_019892.4)[29,30]; and Lyn11-FRB (in pC4RHE, AA 1-11 of Lyn11 (GCIKSKGKDSAGA), AA 2026-2121 of FRB NM_004958.3). Mutations of $G\alpha_q$, hTASK-3, Pseudojanin (C392S of original SAC1) and C-terminal truncations of hTASK-3 were generated using the QuikChange II XL Site-Directed mutagenesis kit (Stratagene, Agilent Technologies, Waldbronn, Germany). For expression in oocytes, human TASK-3 in pSGEM was used. YFP was fused to the N terminus of human PLCβ3 via a 10 AS flexible linker by means of gateway cloning, and the resulting cDNA was cloned into pcDNA3. All constructs were verified by sequencing.

Chemicals. DAG analogues and metabolites (Avanti Polar Lipids, Alabaster, AL, USA) were prepared as 20 mM stock in DMSO. PLC inhibitor U73122 and the inactive analogue U73343 (Sigma-Aldrich) were prepared as 5 mM stock solution in DMSO, kept at −20 °C and diluted into physiological solutions <1 h before experiments. The PLC activator m-3M3FBS and its inactive analogue o-3M3FBS (Tocris Bioscience, Bristol, United Kingdom) were prepared as 50 mM stocks in DMSO. Muscarinic agonist Oxotremorine M (Oxo-M; Tocris Bioscience) was dissolved as 10 mM stock in water. Rapamycin was purchased as 5 mM solution in DMSO (Calbiochem, Merck Chemicals GmbH, Schwalbach, Germany). All drugs were stored at −20 °C and diluted in extracellular solution directly before usage. Inositol-1,4,5-trisphosphate (IP_3; Sigma-Aldrich) was prepared as 5 mM in water and diluted in intracellular solution for excised patch measurements.

Patch-clamp. Whole-cell voltage clamp experiments on CHO dhFr$^-$, $G\alpha_{q/11}{}^{-/-}$ fibroblasts or primary CGNs were performed with an Axopatch 200B amplifier (Molecular Devices, Sunnyvale, CA, USA) controlled by PatchMaster v2x41 software (HEKA, Lambrecht/Pfalz, Germany) via an ITC-16 interface (InstruTECH, HEKA). Currents were low-pass filtered at 2 kHz and sampled at 5 kHz.

Patch pipettes were pulled with a Sutter P-2000 (Sutter Instruments, Novato, CA, USA) from borosilicate glass (Science Products, Hofheim, Germany) to an open pipette resistance of 1.5 to 3 MΩ when filled with pipette solution containing (mM) 135 KCl, 5 Hepes, 5 EGTA, 3.5 $MgCl_2$, 2.5 Na_2ATP, 2.41 $CaCl_2$ and 0.1 Na_2GTP, adjusted to pH 7.3 with KOH. To buffer intracellular Ca^{2+} to effectively zero, the solutions contained (in mM) 85 KCl, 5 Hepes, 20 K_4EGTA or K_4BAPTA, 1 $MgCl_2$, 2.5 Na_2ATP and 0.1 Na_2GTP. Alternatively, intracellular solution contained 5 mM K_4BAPTA with KCl changed to 130 mM. Whole-cell serial resistance was <8 MΩ, which was compensated by 60%. Extracellular solution was composed of (mM) 144 NaCl, 10 HEPES, 5.8 KCl, 5.6 glucose, 1.3 $CaCl_2$, 0.9 $MgCl_2$, 0.7 NaH_2PO_4 and set to pH 7.4 or pH 8.4 (for TASK-1) or pH 5.9 (to block TASK currents) with NaOH. Owing to the development of a cationic current during application of U73122, the extracellular Na^+ was substituted with $NMDG^+$ in the respective recordings.

Giant patch recordings from *Xenopus laevis* oocytes were performed as described previously[54]. In brief, cRNA was synthesized using the mMESSAGE mMACHINE Kit (Ambion, Life Technologies). *Xenopus laevis* oocytes were obtained from EcoCyte Bioscience (Castrop-Rauxel, Germany). Following injection of cRNA, oocytes were incubated at 18 °C for 1–3 days before performing giant patch recordings. Currents were recorded using an EPC10 amplifier (HEKA) controlled by PatchMaster (HEKA), low-pass filtered at 2.9 kHz and sampled at 5 kHz. Giant patch pipettes were fire-polished to obtain open pipette resistances of 0.2–0.5 MΩ when filled with extracellular solution containing (mM) 115 NaCl, 10 HEPES, 5 KCl, 1.5 $CaCl_2$, 1 $MgCl_2$, adjusted to pH 7.4 with NaOH. Patches were excised into intracellular bath solution containing (in mM) 120 KCl, 5 HEPES, 3.5 $MgCl_2$, 1 K_2EGTA and was set to pH 7.2 with KOH. Intracellular solutions were applied to the cytoplasmic face of the patch with a multi-barrel gravity-driven application system. For K^+-free intracellular solution 120 mM NaCl was substituted for KCl. For application of intracellular Ca^{2+}, the K_2EGTA concentration was reduced to 2 mM and 1.98 mM Ca^{2+} was added, yielding 10 µM free Ca^{2+}. In these experiments chloride was substituted by methanesulfonate to minimize currents through Ca^{2+}-activated chloride channels.

All recordings were performed at room temperature (~21 °C). TASK currents were recorded in response to voltage ramps (−100 mV to +50 mV over 500 ms) followed by 200 ms at +50 mV and repeated every 2 s. To quantify current size and time course of current amplitude, currents at +50 mV were averaged for each trace and normalized to the initial current I_0 before drug application. In cerebellar granule cells, the standing outward current, IK_{SO}, was measured at +50 mV after 2.5 s of depolarization to minimize currents through voltage-dependent K^+ channels by inactivation.

TIRF microscopy. TIRF imaging was performed as previously described[55]. In brief, we used a BX51WI upright microscope equipped with a TIRF-condenser (Olympus, Hamburg, Germany), directing a 488-nm laser to obtain total reflection. Fluorescence images were acquired every 4 s with a 530-nm-long-pass emission filter and a CCD camera controlled by TillvisION software (TILL Photonics GmbH, Gräfelfing, Germany). Mean fluorescence intensity F of a single region of interest chosen to cover the majority of the cell's footprint was background subtracted and normalized to the averaged intensity F_0 at the beginning of the experiment or immediately before application of the receptor agonist.

FRET microscopy. Fluorescence resonance energy transfer between $G\alpha_q$-CFP and YFP-PLCβ3 was measured essentially as described[53]. In brief, CHO cells were transiently transfected with $G\alpha_q$-CFP, YFP-PLCβ3, M1R, as well as $G\beta_1$ and $G\gamma_2$, to maintain stoichiometry of heterotrimeric G-proteins[53]. Single whole-cell patch-clamped cells were imaged on a Nikon Eclipse TE2000-U inverted microscope equipped with a Nikon Plan Apo VC 60x/1.40 Oil ∞/0.17 DIC N2 WD 0.13 oil-immersion objective (Nikon GmbH, Düsseldorf, Germany). To avoid fluorophore (YFP) quenching, intracellular chloride was reduced to 60 mM in these experiments with KCl replaced by equimolar K-Aspartate.

The fluorophores were excited using an Oligochrome (Till Photonics, Gräfelfing, Germany), and fluorescence intensities were acquired with fluorescence detection unit (FDU) photodiodes and Oligochrome Imagining Control Unit (ICU FDU-2) (TILL Photonics). CFP was excited through a 430/24 ET bandpass filter. Fluorescence emission intensities were collected using a beam splitter with a 480/40m ET bandpass for CFP (F_{480}) and a 535/30m ET bandpass filter for YFP (F_{535}) (all filters from AHF Analysetechnik AG, Tübingen, Germany). FRET ratio was calculated as F_{535}/F_{480} from background-corrected traces and given as $FRET/FRET_{baseline}$ (relative FRET ratio). Oligochrome control and fluorescence intensity acquisition was performed simultaneous to voltage clamp recordings using an EPC-10 USB patch clamp amplifier in combination with PatchMaster software (HEKA Electronics, Lambrecht, Germany).

Data analysis. Analysis and statistical testing of electrophysiological and imaging data were performed with IGOR Pro (WaveMetrics, Lake Oswego, OR, USA). Data are shown as mean ± s.e.m. with numbers in the summary graphs indicating the number of experiments (individual cells or patches). Unless indicated otherwise, the two-tailed Dunnett's test was used for statistical testing. Asterisks denote the significance level, where *** indicates $P<0.001$, ** indicates $P<0.01$, and * indicates $P<0.05$.

References

1. Brose, N., Betz, A. & Wegmeyer, H. Divergent and convergent signaling by the diacylglycerol second messenger pathway in mammals. *Curr. Opin. Neurobiol.* **14,** 328–340 (2004).
2. Kadamur, G. & Ross, E. M. Mammalian phospholipase C. *Annu. Rev. Physiol.* **75,** 127–154 (2013).
3. Oancea, E. & Meyer, T. Protein kinase C as a molecular machine for decoding calcium and diacylglycerol signals. *Cell* **95,** 307–318 (1998).
4. Carrasco, S. & Merida, I. Diacylglycerol, when simplicity becomes complex. *Trends Biochem. Sci.* **32,** 27–36 (2007).
5. Hurley, J. H. & Misra, S. Signaling and subcellular targeting by membrane-binding domains. *Annu. Rev. Biophys. Biomol. Struct.* **29,** 49–79 (2000).

6. Dietrich, A., Kalwa, H., Rost, B. R. & Gudermann, T. The diacylglycerol-sensitive TRPC3/6/7 subfamily of cation channels: functional characterization and physiological relevance. *Pflugers. Arch.* **451,** 72–80 (2005).
7. Enyedi, P. & Czirjak, G. Molecular background of leak K^+ currents: two-pore domain potassium channels. *Physiol. Rev.* **90,** 559–605 (2010).
8. Brickley, S. G. *et al.* TASK-3 two-pore domain potassium channels enable sustained high-frequency firing in cerebellar granule neurons. *J. Neurosci.* **27,** 9329–9340 (2007).
9. Meuth, S. G. *et al.* Contribution of TWIK-related acid-sensitive K^+ channel 1 (TASK1) and TASK3 channels to the control of activity modes in thalamocortical neurons. *J. Neurosci.* **23,** 6460–6469 (2003).
10. Perrier, J. F., Alaburda, A. & Hounsgaard, J. 5-HT1A receptors increase excitability of spinal motoneurons by inhibiting a TASK-1-like K^+ current in the adult turtle. *J. Physiol.* **548,** 485–492 (2003).
11. Duprat, F. *et al.* TASK, a human background K^+ channel to sense external pH variations near physiological pH. *EMBO J.* **16,** 5464–5471 (1997).
12. Chemin, J. *et al.* Mechanisms underlying excitatory effects of group I metabotropic glutamate receptors via inhibition of 2P domain K^+ channels. *EMBO J.* **22,** 5403–5411 (2003).
13. Mathie, A. Neuronal two-pore-domain potassium channels and their regulation by G protein-coupled receptors. *J. Physiol.* **578,** 377–385 (2007).
14. Talley, E. M. & Bayliss, D. A. Modulation of TASK-1 (Kcnk3) and TASK-3 (Kcnk9) potassium channels: volatile anesthetics and neurotransmitters share a molecular site of action. *J. Biol. Chem.* **277,** 17733–17742 (2002).
15. Talley, E. M., Lei, Q., Sirois, J. E. & Bayliss, D. A. TASK-1, a two-pore domain K^+ channel, is modulated by multiple neurotransmitters in motoneurons. *Neuron* **25,** 399–410 (2000).
16. Lazarenko, R. M. *et al.* Motoneuronal TASK channels contribute to immobilizing effects of inhalational general anesthetics. *J. Neurosci.* **30,** 7691–7704 (2010).
17. Bandulik, S., Penton, D., Barhanin, J. & Warth, R. TASK1 and TASK3 potassium channels: determinants of aldosterone secretion and adrenocortical zonation. *Horm. Metab. Res.* **42,** 450–457 (2010).
18. Chen, X. *et al.* Inhibition of a background potassium channel by Gq protein α-subunits. *Proc. Natl Acad. Sci. USA* **103,** 3422–3427 (2006).
19. Schiekel, J. *et al.* The inhibition of the potassium channel TASK-1 in rat cardiac muscle by endothelin-1 is mediated by phospholipase C. *Cardiovasc. Res.* **97,** 97–105 (2013).
20. Horowitz, L. F. *et al.* Phospholipase C in living cells: activation, inhibition, Ca^{2+} requirement, and regulation of M current. *J. Gen. Physiol.* **126,** 243–262 (2005).
21. Boyd, D. F., Millar, J. A., Watkins, C. S. & Mathie, A. The role of Ca^{2+} stores in the muscarinic inhibition of the K+ current IK(SO) in neonatal rat cerebellar granule cells. *J. Physiol.* **529**(Pt 2): 321–331 (2000).
22. Czirjak, G., Petheo, G. L., Spat, A. & Enyedi, P. Inhibition of TASK-1 potassium channel by phospholipase C. *Am. J. Physiol. Cell Physiol.* **281,** C700–C708 (2001).
23. Stauffer, T. P., Ahn, S. & Meyer, T. Receptor-induced transient reduction in plasma membrane PtdIns(4,5)P_2 concentration monitored in living cells. *Curr. Biol.* **8,** 343–346 (1998).
24. Varnai, P. & Balla, T. Visualization of phosphoinositides that bind pleckstrin homology domains: calcium- and agonist-induced dynamic changes and relationship to Myo-[3H]inositol-labeled phosphoinositide pools. *J. Cell Biol.* **143,** 501–510 (1998).
25. Oancea, E., Teruel, M. N., Quest, A. F. & Meyer, T. Green fluorescent protein (GFP)-tagged cysteine-rich domains from protein kinase C as fluorescent indicators for diacylglycerol signaling in living cells. *J. Cell Biol.* **140,** 485–498 (1998).
26. Venkatakrishnan, G. & Exton, J. H. Identification of determinants in the α-subunit of G_q required for phospholipase C activation. *J. Biol. Chem.* **271,** 5066–5072 (1996).
27. Zhang, X. *et al.* Direct inhibition of the cold-activated TRPM8 ion channel by $G\alpha_q$. *Nat. Cell Biol.* **14,** 851–858 (2012).
28. Lopes, C. M. B. *et al.* PIP_2 hydrolysis underlies agonist-induced inhibition and regulates voltage gating of two-pore domain K^+ channels. *J. Physiol.* **564,** 117–129 (2005).
29. Lindner, M., Leitner, M. G., Halaszovich, C. R., Hammond, G. R. & Oliver, D. Probing the regulation of TASK potassium channels by PI(4,5)P_2 with switchable phosphoinositide phosphatases. *J. Physiol.* **589,** 3149–3162 (2011).
30. Hammond, G. R. *et al.* PI4P and PI(4,5)P_2 are essential but independent lipid determinants of membrane identity. *Science* **337,** 727–730 (2012).
31. Suh, B.-C., Inoue, T., Meyer, T. & Hille, B. Rapid chemically induced changes of PtdIns(4,5)P_2 gate KCNQ ion channels. *Science* **314,** 1454–1457 (2006).
32. Bae, Y. S. *et al.* Identification of a compound that directly stimulates phospholipase C activity. *Mol. Pharmacol.* **63,** 1043–1050 (2003).
33. Hodgkin, M. N. *et al.* Diacylglycerols and phosphatidates: which molecular species are intracellular messengers? *Trends Biochem. Sci.* **23,** 200–204 (1998).
34. Maingret, F., Patel, A. J., Lazdunski, M. & Honore, E. The endocannabinoid anandamide is a direct and selective blocker of the background K^+ channel TASK-1. *EMBO J.* **20,** 47–54 (2001).
35. Reisenberg, M., Singh, P. K., Williams, G. & Doherty, P. The diacylglycerol lipases: structure, regulation and roles in and beyond endocannabinoid signalling. *Philos. Trans. R. Soc. Lond. B. Biol. Sci.* **367,** 3264–3275 (2012).
36. Aller, M. I. *et al.* Modifying the subunit composition of TASK channels alters the modulation of a leak conductance in cerebellar granule neurons. *J. Neurosci.* **25,** 11455–11467 (2005).
37. Kang, D., Han, J., Talley, E. M., Bayliss, D. A. & Kim, D. Functional expression of TASK-1/TASK-3 heteromers in cerebellar granule cells. *J. Physiol.* **554,** 64–77 (2004).
38. Millar, J. A. *et al.* A functional role for the two-pore domain potassium channel TASK-1 in cerebellar granule neurons. *Proc. Natl Acad. Sci. USA* **97,** 3614–3618 (2000).
39. Watkins, C. S. & Mathie, A. A non-inactivating K^+ current sensitive to muscarinic receptor activation in rat cultured cerebellar granule neurons. *J. Physiol.* **491,** 401–412 (1996).
40. Han, J., Truell, J., Gnatenco, C. & Kim, D. Characterization of four types of background potassium channels in rat cerebellar granule neurons. *J. Physiol.* **542,** 431–444 (2002).
41. Veale, E. L. *et al.* $G\alpha_q$-mediated regulation of TASK3 two-pore domain potassium channels: the role of protein kinase C. *Mol. Pharmacol.* **71,** 1666–1675 (2007).
42. Veale, E. L., Buswell, R., Clarke, C. E. & Mathie, A. Identification of a region in the TASK3 two pore domain potassium channel that is critical for its blockade by methanandamide. *Br. J. Pharmacol.* **152,** 778–786 (2007).
43. Bautista, D. M. *et al.* Pungent agents from Szechuan peppers excite sensory neurons by inhibiting two-pore potassium channels. *Nat. Neurosci.* **11,** 772–779 (2008).
44. Hofmann, T. *et al.* Direct activation of human TRPC6 and TRPC3 channels by diacylglycerol. *Nature* **397,** 259–263 (1999).
45. Chemin, J. *et al.* A phospholipid sensor controls mechanogating of the K^+ channel TREK-1. *EMBO J.* **24,** 44–53 (2005).
46. Honore, E., Maingret, F., Lazdunski, M. & Patel, A. J. An intracellular proton sensor commands lipid- and mechano-gating of the K^+ channel TREK-1. *EMBO J.* **21,** 2968–2976 (2002).
47. Sandoz, G., Bell, S. C. & Isacoff, E. Y. Optical probing of a dynamic membrane interaction that regulates the TREK1 channel. *Proc. Natl Acad. Sci. USA* **108,** 2605–2610 (2011).
48. Ashmole, I. *et al.* The response of the tandem pore potassium channel TASK-3 (K(2P)9.1) to voltage: gating at the cytoplasmic mouth. *J. Physiol.* **587,** 4769–4783 (2009).
49. Shulga, Y. V., Topham, M. K. & Epand, R. M. Regulation and functions of diacylglycerol kinases. *Chem. Rev.* **111,** 6186–6208 (2011).
50. Leach, N. T. *et al.* Disruption of diacylglycerol kinase delta (DGKD) associated with seizures in humans and mice. *Am. J. Hum. Genet.* **80,** 792–799 (2007).
51. Kakefuda, K. *et al.* Diacylglycerol kinase β knockout mice exhibit lithium-sensitive behavioral abnormalities. *PLoS ONE* **5,** e13447 (2010).
52. Rodriguez de Turco, E. B. *et al.* Diacylglycerol kinase epsilon regulates seizure susceptibility and long-term potentiation through arachidonoyl- inositol lipid signaling. *Proc. Natl Acad. Sci. USA* **98,** 4740–4745 (2001).
53. Bodmann, E. L. *et al.* Dynamics of $G\alpha_q$-protein-p63RhoGEF interaction and its regulation by RGS2. *Biochem. J.* **458,** 131–140 (2014).
54. Oliver, D. *et al.* Functional conversion between A-type and delayed rectifier K^+ channels by membrane lipids. *Science* **304,** 265–270 (2004).
55. Halaszovich, C. R., Schreiber, D. N. & Oliver, D. Ci-VSP is a depolarization-activated phosphatidylinositol-4,5-bisphosphate and phosphatidylinositol-3,4,5-trisphosphate 5'-phosphatase. *J. Biol. Chem.* **284,** 2106–2113 (2009).

Acknowledgements

We thank Drs J. Daut, J. Oberwinkler and T. Budde for helpful discussions and critical reading of the manuscript, and M. Bertoune for help with establishing granule neuron cultures. This work was supported by grants from the Deutsche Forschungsgemeinschaft to D.O. (FOR 1086 OL 240/3-1 and SFB 593 TP12).

Author contributions

D.O. and B.U.W. conceived the study; B.U.W., M.L., L.G., A.A., Y.K. and M.G.L. performed experiments and analysed data; D.O. analysed data; M.B. developed the FRET assay; D.O. and B.U.W. wrote the manuscript.

Additional information

Competing financial interests: The authors declare no competing financial interests.

Reprints and permission information is available online at http://npg.nature.com/reprintsandpermissions/

How to cite this article: Wilke, B. U. *et al.* Diacylglycerol mediates regulation of TASK potassium channels by Gq-coupled receptors. *Nat. Commun.* 5:5540 doi: 10.1038/ncomms6540 (2014).

8 Appendix

8.1. Verzeichnis der akademischen Lehrer

Meine akademischen Lehrer waren die Damen und Herren in Marburg…

Aigner, Bastians, Bauer, Bertoune, Bette, Brehm, Bünemann, Bremmer, Cetin, Daut, Decher, Del Rey, Elsässer, Hassel, Huber, Jacob, , Koolman, Leitner, Lill, Lillig, Lohöfer, Lohhoff, Maisner, Müller, Müller-Brüsselbach, Oberwinkler, Oliver, Pagenstecher, Plant, Preißig-Müller, Röhm, Schäfer, Schulz, Schütz, Suske, Weihe, Westermann, Wrocklage; Yu

sowie an anderen Orten…

Fakler (Freiburg), Rämet (Tampere, Finnland)

8.2. Danksagung

Hier möchte ich allen danken, die diese Arbeit möglich gemacht haben.

Besonders danken möchte ich Dominik, durch dessen Ideen dieses Projekt entstanden ist, und der – angefangen von Finanzierung, Wissen, Begeisterung, Laborplatz, Gelder für alles Nötige, Patchsetup, diverser Mikroskope, Manpower bis zu seiner seine eigenen Zeit und Geduld - alles für die Projektdurchführung bereitgestellt hat. Außerdem möchte ich ihm auch dafür danken, dass er wohl der netteste und verständnisvollste Chef ist, was das Arbeiten für und mit ihm sehr angenehm gemacht hat.

Außerdem möchte ich mich bei allen in der Arbeitsgruppe bedanken, die mir während der Zeit im Labor so viel geholfen haben und dafür gesorgt haben, dass ich jeden Tag gerne ins Institut geradelt bin. Ein besonderer Dank geht an Michael für die Unterstützung bei allen elektrophysiologischen und technischen Problemen und für die große Hilfe in meinem Projekt und bei der Erstellung dieser Arbeit. Danke auch an Christian für die Hilfe mit Programmen und Geräten. Danke an Moritz für die Arbeiten zu dem Projekt. Danke an Olga, Sigrid, Natalia und Julia für die liebevolle Pflege der CHO Zellen sowie Gisela und Eva für die Bereitstellung der DNA in rauen Mengen. Ein lieber Dank an Aileen, Angeliki, Anja, Dmitry, Florian, Julia, Kirstin, Marlen, Michael, Vijay und Vroni für die unterhaltsamen Pausen und Tipps zwischendurch. Ebenso bedanke ich mich bei allen anderen netten Menschen aus der AG Oliver und dem Institut, die für ein gutes Arbeitsklima gesorgt haben, besonders den hilfsbereiten Männern aus der Feinmechanischen und Elektronischen Werkstatt, die beim Grillen eine genauso große Unterstützung waren wie bei der Wiederbelebung der Kaffeemaschine und dem Bau des perfekten Setups dank hundertstel Millimeter genauen Bohrungen in Plexiglas und Edelstahl.

Danke an all meine Freunde, die mich Teile meines Lebens, Studiums und meiner Doktorarbeitszeit in Marburg begleitet haben und mich zum Glück erst jetzt in Marburg zurückgelassen haben (zumindest die meisten davon).

Ein großer Dank geht natürlich auch an meine tollen Eltern, die mich bei allem immerzu unterstützt haben. Genauso hatte meine liebe Schwester Bine 29 schöne Jahre ein offenes Ohr für mich und war mir stets auch eine sehr gute Freundin. Auch ein Dank an Fabian, dass es mich (fast) nie geärgert hat und nicht verhindert hat, diese Arbeit fertigzustellen (dabei waren Gesa und Peter sicher nicht ganz unbeteiligt – danke auch ihnen).

Und natürlich möchte ich Michael danken… für alles!